# Elements of Applied Bifurcation Theory, Second Edition

*Yuri A. Kuznetsov*

**Springer**

# 6

# Bifurcations of Orbits Homoclinic and Heteroclinic to Hyperbolic Equilibria

In this chapter we will study global bifurcations corresponding to the appearance of *homoclinic* or *heteroclinic* orbits connecting hyperbolic equilibria in continuous-time dynamical systems. First we consider in detail two- and three-dimensional cases where geometrical intuition can be fully exploited. Then we show how to reduce generic $n$-dimensional cases to the considered ones plus a four-dimensional case. This remaining case is treated in Appendix 1.

## 6.1 Homoclinic and heteroclinic orbits

Consider a continuous-time dynamical system $\{\mathbb{R}^1, \mathbb{R}^n, \varphi^t\}$ defined by a system of ODEs

$$\dot{x} = f(x), \quad x = (x_1, x_2, \ldots, x_n)^T \in \mathbb{R}^n, \tag{6.1}$$

where $f$ is smooth. Let $x_0, x_{(1)}$, and $x_{(2)}$ be equilibria of the system.

**Definition 6.1** *An orbit* $\Gamma_0$ *starting at a point* $x \in \mathbb{R}^n$ *is called* homoclinic *to the equilibrium point* $x_0$ *of system* (6.1) *if* $\varphi^t x \to x_0$ *as* $t \to \pm\infty$.

**Definition 6.2** *An orbit* $\Gamma_0$ *starting at a point* $x \in \mathbb{R}^n$ *is called* heteroclinic *to the equilibrium points* $x_{(1)}$ *and* $x_{(2)}$ *of system* (6.1) *if* $\varphi^t x \to x_{(1)}$ *as* $t \to -\infty$ *and* $\varphi^t x \to x_{(2)}$ *as* $t \to +\infty$.

Figure 6.1 shows examples of homoclinic and heteroclinic orbits to saddle points if $n = 2$, while Figure 6.2 presents relevant examples for $n = 3$.

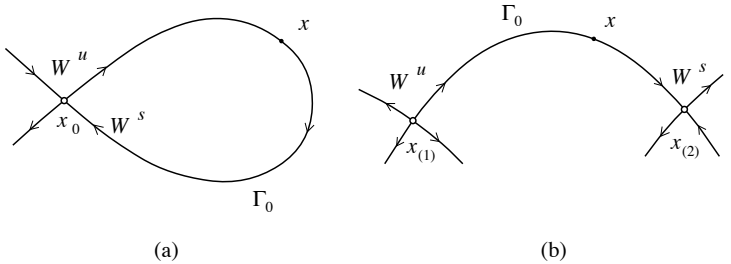


FIGURE 6.1. (a) Homoclinic and (b) heteroclinic orbits on the plane.

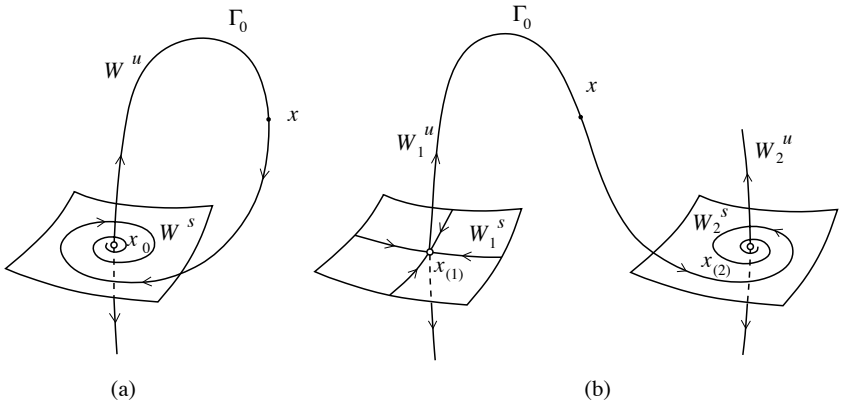


FIGURE 6.2. (a) Homoclinic and (b) heteroclinic orbits in three-dimensional space.

It is clear that a homoclinic orbit $\Gamma_0$ to the equilibrium $x_0$ belongs to the intersection of its unstable and stable sets: $\Gamma_0 \subset W^u(x_0) \cap W^s(x_0)$. Similarly, a heteroclinic orbit $\Gamma_0$ to the equilibria $x_{(1)}$ and $x_{(2)}$ satisfies $\Gamma_0 \subset W^u(x_{(1)}) \cap W^s(x_{(2)})$. It should be noticed that the Definitions 6.1 and 6.2 do not require the equilibria to be hyperbolic. Figure 6.3 shows, for example, a homoclinic orbit to a saddle-node point with an eigenvalue $\lambda_1 = 0$. Actually, orbits homoclinic to hyperbolic equilibria are of particular interest since their presence results in structural instability while the equilibria themselves are structurally stable.

**Lemma 6.1** *A homoclinic orbit to a hyperbolic equilibrium of* (6.1) *is structurally unstable.* □

This lemma means that we can perturb a system with an orbit $\Gamma_0$ that is homoclinic to $x_0$ such that the phase portrait in a neighborhood of $\Gamma_0 \cup x_0$ becomes topologically nonequivalent to the original one. As we shall see, the homoclinic orbit simply disappears for generic $C^1$ perturbations of the system. This is a bifurcation of the phase portrait.

To prove the lemma, we need a small portion of transversality theory.

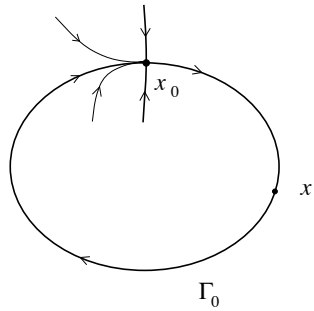


FIGURE 6.3. Homoclinic orbit $\Gamma_0$ to a saddle-node equilibrium.

**Definition 6.3** *Two smooth manifolds $M, N \subset \mathbb{R}^n$ intersect* transversally *if there exist $n$ linearly independent vectors that are tangent to at least one of these manifolds at any intersection point.*

For example, a surface and a curve intersecting with a nonzero angle at some point in $\mathbb{R}^3$ are transversal. The main property of transversal intersection is that it persists under small $C^1$ perturbations of the manifolds. In other words, if manifolds $M$ and $N$ intersect transversally, so will all sufficiently $C^1$-close manifolds. Conversely, if the manifolds intersect nontransversally, generic perturbations make them either nonintersecting or transversally intersecting.

Since in this chapter we deal exclusively with saddle (or saddle-focus) hyperbolic equilibria, the sets $W^u$ and $W^s$ are smooth (immersed) invariant manifolds.[1] Any sufficiently $C^1$-close system has a nearby saddle point, and its invariant manifolds $W^{u,s}$ are $C^1$-close to the corresponding original ones in a neighborhood of the saddle.

**Proof of Lemma 6.1:**

Suppose that system (6.1) has a hyperbolic equilibrium $x_0$ with $n_+$ eigenvalues having positive real parts and $n_-$ eigenvalues having negative real parts, $n_\pm > 0$, $n_+ + n_- = n$. Assume that the corresponding stable and unstable manifolds $W^u(x_0)$ and $W^s(x_0)$ intersect along a homoclinic orbit. To prove the lemma, we shall show that the intersection cannot be transversal. Indeed, at any point $x$ of this orbit, the vector $f(x)$ is tangent to both manifolds $W^u(x_0)$ and $W^s(x_0)$. Therefore, we can find no more than $n_+ + n_- - 1 = n - 1$ independent tangent vectors to these manifolds, since $\dim W^u = n_+$, $\dim W^s = n_-$. Moreover, any generic perturbation of (6.1) splits the manifolds in that remaining direction and they do not intersect anymore near $\Gamma_0$. □

[1] Meanwhile, the manifolds $W^u(x_0)$ and $W^s(x_0)$ intersect transversally at $x_0$.

Let us characterize the behavior of the stable and unstable manifolds near homoclinic bifurcations in two- and three-dimensional systems in more detail.

*Case* $n = 2$. Consider a planar system having a homoclinic orbit to a saddle $x_0$, as shown in the central part of Figure 6.4. Introduce a one-

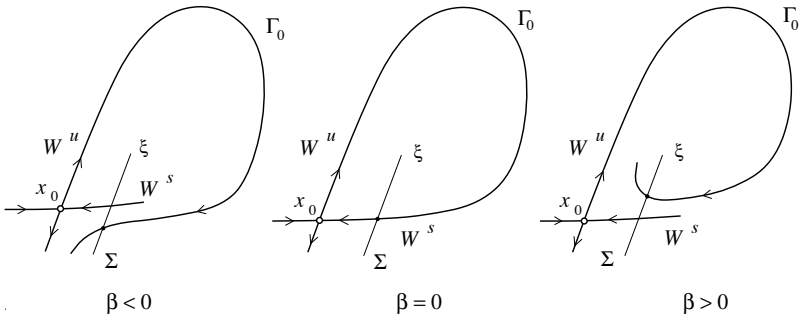


FIGURE 6.4. Split function in the planar case ($n = 2$).

dimensional local cross-section $\Sigma$ to the stable manifold $W^s(x_0)$ near the saddle, as shown in the figure. Select a coordinate $\xi$ along $\Sigma$ such that the point of the intersection with the stable manifold corresponds to $\xi = 0$. This construction can be carried out for all sufficiently close systems. For such systems, however, the unstable manifold $W^u$ generically does not return to the saddle. Figure 6.4 illustrates the two possibilities: The manifolds split either "down" or "up." Denote by $\xi^u$ the $\xi$-value of the intersection of $W^u$ with $\Sigma$.

**Definition 6.4** *The scalar* $\beta = \xi^u$ *is called a* split function.

Actually, the split function is a *functional* defined on the original and perturbed systems. It becomes a smooth function of parameters for a parameter-dependent system. The equation

$$\beta = 0$$

is a bifurcation condition for the homoclinic bifurcation in $\mathbb{R}^2$. Thus, the homoclinic bifurcation in this case has codimension *one*.

**Remark:**

There is a constructive proof of Lemma 6.1 in the planar case due to Andronov. A one-parameter perturbation destroying the homoclinic (heteroclinic) orbit can be constructed explicitly. For example, if a system

$$\begin{cases} \dot{x}_1 &= f_1(x_1, x_2), \\ \dot{x}_2 &= f_2(x_1, x_2), \end{cases} \tag{6.2}$$

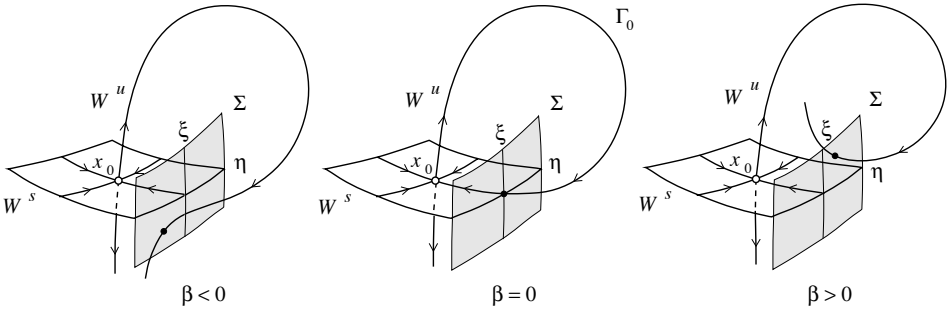


FIGURE 6.5. Split function in the case $n = 3$.

has a homoclinic orbit to a saddle, then the system

$$\begin{cases} \dot{x}_1 &= f_1(x_1, x_2) - \alpha f_2(x_1, x_2), \\ \dot{x}_2 &= \alpha f_1(x_1, x_2) + f_2(x_1, x_2), \end{cases} \tag{6.3}$$

has no nearby homoclinic orbits to this saddle for any sufficiently small $|\alpha| \neq 0$. System (6.3) is obtained from (6.2) by a *rotation of the vector field*. The proof is left as an exercise to the reader. $\diamondsuit$

*Case* $n = 3$. It is also possible to define a split function in this case. Consider a system in $\mathbb{R}^3$ with a homoclinic orbit $\Gamma_0$ to a saddle $x_0$. Assume that $\dim W^u = 1$ (otherwise, reverse the time direction), and introduce a two-dimensional cross-section $\Sigma$ with coordinates $(\xi, \eta)$ as in Figure 6.5. Suppose that $\xi = 0$ corresponds to the intersection of $\Sigma$ with the stable manifold $W^s$ of $x_0$. As before, this can be done for all sufficiently close systems. Let the point $(\xi^u, \eta^u)$ correspond to the intersection of $W^u$ with $\Sigma$. Then, a split function can be defined as in the planar case before: $\beta = \xi^u$. Its zero

$$\beta = 0$$

gives a condition for the homoclinic bifurcation in $\mathbb{R}^3$.

**Remarks:**

(1) The preceding cases are examples of nontransversal intersections of the invariant manifolds $W^u$ and $W^s$. One can construct a three-dimensional system with a structurally stable *heteroclinic* orbit connecting two saddles: This orbit must be a transversal intersection of the corresponding *two-dimensional* stable and unstable manifolds.

(2) There are particular classes of dynamical systems (such as Hamiltonian) for which the presence of a nontransversal homoclinic orbit is generic. $\diamondsuit$

Thus, we have found that under certain conditions the presence of a homo-/hetero-clinic orbit $\Gamma_0$ to a saddle/saddles implies a bifurcation. Our

goal in the next sections will be to describe the phase portrait bifurcations near such an orbit under small $C^1$ perturbations of the system. "Near" means in a sufficiently small neighborhood $U_0$ of $\Gamma_0 \cup x_0$ or $\Gamma_0 \cup x_{(1)} \cup x_{(2)}$. This task is more complex than for bifurcations of equilibria since it is not easy to construct a continuous-time system that would be a topological normal form for the bifurcation. In some cases ahead, all one-parameter systems satisfying some generic conditions are topologically equivalent in a neighborhood of the corresponding homoclinic bifurcation. In these cases, we will characterize the relevant universal bifurcation diagram by drawing key orbits of the corresponding phase portraits. This will completely describe the diagram up to topological equivalence.

Unfortunately, there are more involved cases in which such an equivalence is absent. In these cases no universal bifurcation diagrams can be presented. Nevertheless, topologically nonequivalent bifurcation diagrams reveal some features in common, and we will give schematic phase portraits describing the bifurcation for such cases as well.

The nontransversal heteroclinic case is somehow trivial since the disappearance of the connecting orbit is the only essential event in $U_0$ (see Figure 6.6). Therefore, in this chapter we will focus on the homoclinic orbit bifurcations and return to nonhyperbolic homoclinic orbits and their associated bifurcations in Chapter 7.

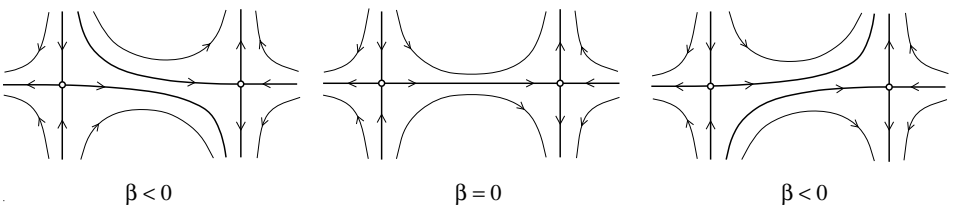


FIGURE 6.6. Heteroclinic bifurcation on the plane.

## 6.2 Andronov-Leontovich theorem

In the planar case, the homoclinic bifurcation is completely characterized by the following theorem.

**Theorem 6.1 (Andronov & Leontovich [1939])** *Consider a two-dimensional system*

$$\dot{x} = f(x, \alpha), \quad x \in \mathbb{R}^2, \ \alpha \in \mathbb{R}^1, \tag{6.4}$$

*with smooth $f$, having at $\alpha = 0$ a saddle equilibrium point $x_0 = 0$ with eigenvalues $\lambda_1(0) < 0 < \lambda_2(0)$ and a homoclinic orbit $\Gamma_0$. Assume the following genericity conditions hold:*

(H.1) $\sigma_0 = \lambda_1(0) + \lambda_2(0) \neq 0$;

(H.2) $\beta'(0) \neq 0$, *where* $\beta(\alpha)$ *is the previously defined split function.*

*Then, for all sufficiently small* $|\alpha|$, *there exists a neighborhood* $U_0$ *of* $\Gamma_0 \cup x_0$ *in which a unique limit cycle* $L_\beta$ *bifurcates from* $\Gamma_0$. *Moreover, the cycle is stable and exists for* $\beta > 0$ *if* $\sigma_0 < 0$, *and is unstable and exists for* $\beta < 0$ *if* $\sigma_0 > 0$.

The following definition is quite useful.

**Definition 6.5** *The real number* $\sigma = \lambda_1 + \lambda_2$ *is called the* saddle quantity.

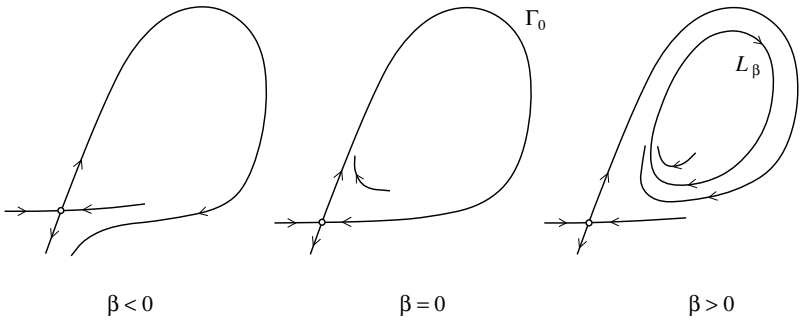


FIGURE 6.7. Homoclinic bifurcation on the plane ($\sigma_0 < 0$).

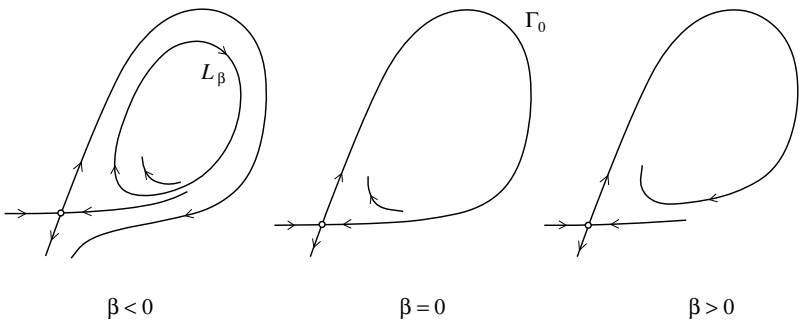


FIGURE 6.8. Homoclinic bifurcation on the plane ($\sigma_0 > 0$).

Figures 6.7 and 6.8 illustrate the above theorem. If $\alpha = 0$, the system has an orbit homoclinic to the origin. A saddle equilibrium point exists near the origin for all sufficiently small $|\alpha| \neq 0$, while the homoclinic orbit disappears, splitting "up" or "down." According to condition (H.2), the split function $\beta = \beta(\alpha)$ can be considered as a new parameter.

If the saddle quantity satisfies $\sigma_0 < 0$, the homoclinic orbit at $\beta = 0$ is *stable from the inside*, and the theorem gives the existence of a unique and stable limit cycle $L_\beta \subset U_0$ for $\beta > 0$. For $\beta < 0$ there are no periodic orbits in $U_0$. If the saddle quantity satisfies $\sigma_0 > 0$, the homoclinic orbit at $\beta = 0$ is *unstable from the inside*, and the theorem gives the existence of

a unique but unstable limit cycle $L_\beta \subset U_0$ for $\beta < 0$. For $\beta > 0$ there are no periodic orbits in $U_0$. Thus, the sign of $\sigma_0$ determines the direction of bifurcation and the stability of the appearing limit cycle. As usual, the term "direction" has a conventional meaning and is related to our definition of the split function.

As $|\beta| \to 0$, the cycle passes closer and closer to the saddle and becomes increasingly "angled" (see Figure 6.9). Its period $T_\beta$ tends to infinity as $\beta$

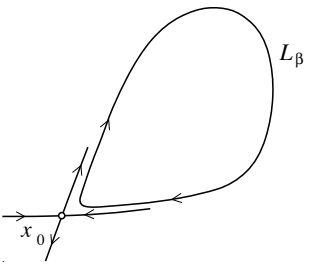


FIGURE 6.9. A cycle near a homoclinic bifurcation.

approaches zero since a phase point moving along the cycle spends more and more time near the equilibrium (see Figure 6.10). The corresponding

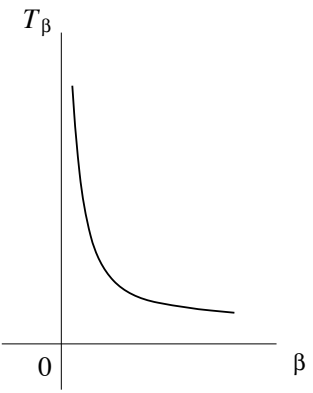


FIGURE 6.10. Period of the cycle near a homoclinic bifurcation.

time series $(x_1(t), x_2(t))$ demonstrates "peaks" of finite length interspersed by very long "near-equilibrium" intervals.

**Proof of Theorem 6.1:**

The main idea of the proof is to introduce two local cross-sections near the saddle, $\Sigma$ and $\Pi$, which are transversal to the stable and the unstable manifolds, respectively (see Figure 6.11). Then it is possible to define a Poincaré map $P$ on a half-section $\Sigma^+$,

$$P : \Sigma^+ \to \Sigma,$$

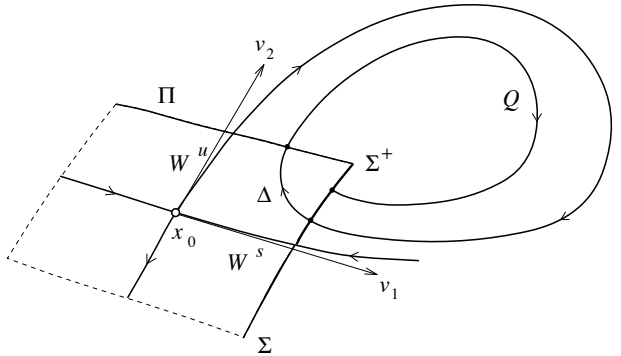


FIGURE 6.11. Poincaré map for homoclinic bifurcation on the plane.

as a superposition of a near-to-saddle map $\Delta : \Sigma^+ \to \Pi$ and a map $Q : \Pi \to \Sigma$ near the global part of the homoclinic orbit:

$$P = Q \circ \Delta.$$

Finally, we have to take into account the usual correspondence between limit cycles of (6.4) and fixed points of $P$. The proof proceeds through several steps.

*Step 1* (*Introduction of eigenbasis coordinates*). Without loss of generality, assume that the origin is a saddle equilibrium of (6.4) for all sufficiently small $|\alpha|$. We consider $\beta$ as a new parameter but do not indicate the parameter dependence for a while in order to simplify notation.

There is an invertible linear coordinate transformation that allows us to write (6.4) in the form

$$\left\{ \begin{array}{rcl} \dot{x}_1 & = & \lambda_1 x_1 + g_1(x_1, x_2), \\ \dot{x}_2 & = & \lambda_2 x_2 + g_2(x_1, x_2), \end{array} \right. \tag{6.5}$$

where $x_{1,2}$ denote the new coordinates and $g_{1,2}$ are smooth $O(\|x\|^2)$-functions, $x = (x_1, x_2)^T$, $\|x\|^2 = x_1^2 + x_2^2$.

*Step 2* (*Local linearization of the invariant manifolds*). According to the Local Stable Manifold Theorem (see Chapter 3), the stable and unstable invariant manifolds $W^s$ and $W^u$ of the saddle exist and have the local representations

$$\begin{array}{l} W^s : \ x_2 = S(x_1), \ S(0) = S'(0) = 0; \\ W^u : \ x_1 = U(x_2), \ U(0) = U'(0) = 0, \end{array}$$

with smooth $S, U$ (see Figure 6.12). Introduce new variables $y = (y_1, y_2)^T$ near the saddle:

$$\left\{ \begin{array}{rcl} y_1 & = & x_1 - U(x_2), \\ y_2 & = & x_2 - S(x_1). \end{array} \right.$$

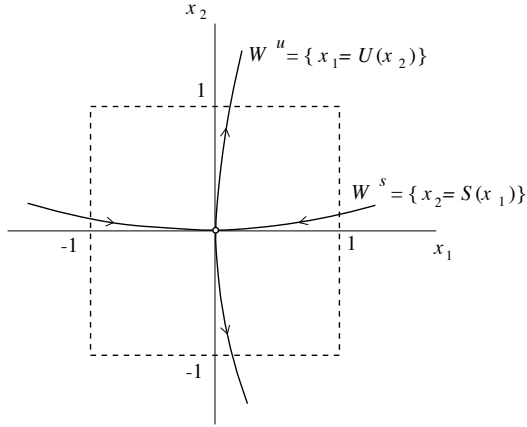


FIGURE 6.12. Local stable and unstable manifolds in $x$-coordinates.

This coordinate change is smooth and invertible in some neighborhood of the origin.[2] We can assume that this neighborhood contains the unit square $\Omega = \{y : -1 < y_{1,2} < 1\}$, which is a matter of an additional linear scaling of system (6.5). Thus, system (6.5) in the new coordinates takes in $\Omega$ the form

$$\begin{cases} \dot{y}_1 &= \lambda_1 y_1 + y_1 h_1(y_1, y_2), \\ \dot{y}_2 &= \lambda_2 y_2 + y_2 h_2(y_1, y_2), \end{cases} \tag{6.6}$$

where $h_{1,2} = O(\|y\|)$. Notice that (6.6) is a *nonlinear* smooth system with a saddle at the origin whose invariant manifolds are linear and coincide with the coordinate axes in $\Omega$ (see Figure 6.13).

*Step 3* (*Local $C^1$-linearization of the system*). Now introduce new coordinates $(\xi, \eta)$ in $\Omega$ in which system (6.6) becomes *linear*:

$$\begin{cases} \dot{\xi} &= \lambda_1 \xi, \\ \dot{\eta} &= \lambda_2 \eta. \end{cases} \tag{6.7}$$

More precisely, we show that the flow corresponding to (6.6) is $C^1$-equivalent in $\Omega$ to the flow generated by the linear system (6.7). To construct the conjugating map

$$\begin{cases} \xi &= \varphi(y_1, y_2), \\ \eta &= \psi(y_1, y_2), \end{cases}$$

we use the following geometric construction. Take a point $y = (y_1, y_2) \in \Omega$ and the orbit passing through this point (see Figure 6.14(a)). Let $\tau_1$ and $\tau_2$ be the absolute values of the positive and negative times required

[2] To be more precise, we have to consider a *global* invertible smooth change of the coordinates that coincides with the specified one in a neighborhood of the saddle and is the identity outside some other neighborhood of the saddle. The same should be noticed concerning the map $\Phi$ to be constructed later.

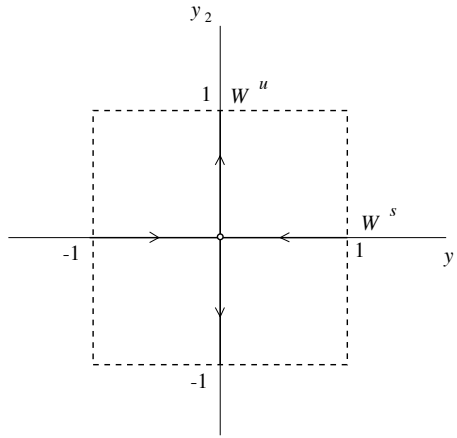


FIGURE 6.13. Locally linearized stable and unstable manifolds in $y$-coordinates.

for such an orbit to reach the boundary of $\Omega$ in system (6.6). It can be checked (Exercise 7(a)) that the pair $(\tau_1, \tau_2)$ is uniquely defined for $y \neq 0$ within each quadrant of $\Omega$.[3] Now find a point $(\xi, \eta)$ in the same quadrant of $\Omega$ with the same "exit" times $\tau_1$ and $\tau_2$ for the corresponding orbit of (6.7) (see Figure 6.14(b)). Let us take $\xi = \eta = 0$ for $y = 0$. Thus,

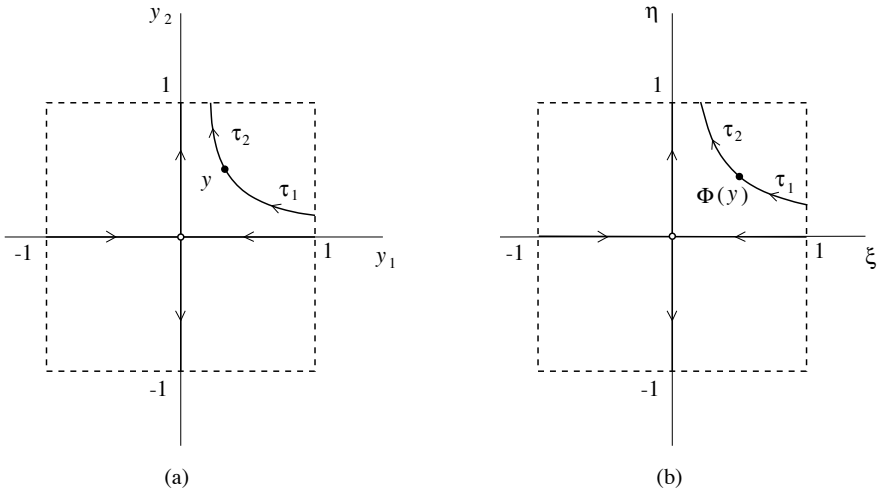


FIGURE 6.14. Construction of $C^1$-equivalence.

a map $\Phi : (y_1, y_2) \mapsto (\xi, \eta)$ is constructed. It clearly maps orbits of the nonlinear system (6.6) into orbits of the linear system (6.7), preserving time parametrization. Map $\Phi : \Omega \to \Omega$ is a homeomorphism transforming

[3]For points on the coordinate axes we allow one of $\tau_{1,2}$ to be equal to $\pm\infty$.

each component of the boundary of $\Omega$ into itself; it is identical along the axes. To define a useful coordinate change it must be at least continuously differentiable in $\Omega$. Indeed, the map $\Phi$ is a $C^1$ map. Actually, it is smooth away from the origin but has only first-order continuous partial derivatives at $y = 0$ (the relevant calculations are left to the reader as Exercise 7(b)).

*Step 4* (*Analysis of the superposition*). Using the new coordinates $(\xi, \eta)$, we can compute the near-to-saddle map *analytically*. We can assume that the cross-section $\Sigma$ has the representation $\xi = 1, -1 \le \eta \le 1$. Then, $\eta$ can be used as a coordinate on it, and $\Sigma^+$ is defined by $\xi = 1, 0 \le \eta \le 1$. The map acts from $\Sigma^+$ into a cross-section $\Pi$, which is defined by $\eta = 1, -1 \le \xi \le 1$, and has $\xi$ as a coordinate (see Figure 6.15). Integrating the linear system (6.7), we obtain

$$\Delta : \ \xi = \eta^{-\frac{\lambda_1}{\lambda_2}}.$$

Notice that the resulting map is *nonlinear* regardless of the linearity of system (6.7). We assumed $\xi = 0$ for $\eta = 0$ by continuity.

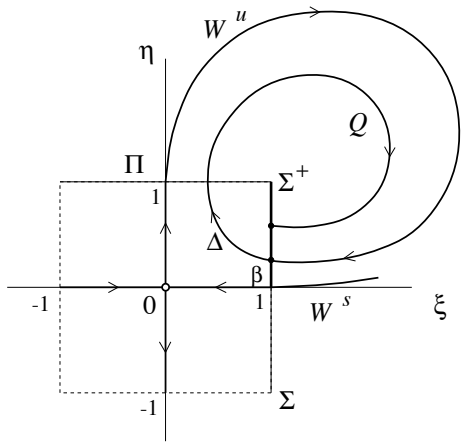


FIGURE 6.15. Poincaré map in locally linearizing coordinates.

The global map expressed in $\xi$ and $\eta$ is continuously differentiable and invertible and has the following general form:

$$Q : \ \eta = \beta + a\xi + O(\xi^2),$$

where $\beta$ is the split function and $a > 0$ since the orbits cannot intersect. Actually, $\lambda_{1,2} = \lambda_{1,2}(\beta)$, $a = a(\beta)$, but as we shall see below only values at $\beta = 0$ are relevant. Fixed points with small $|\eta|$ of the Poincaré map

$$P : \eta \mapsto \beta + a\eta^{-\frac{\lambda_1}{\lambda_2}} + \cdots$$

can be easily analyzed for small $|\beta|$ (see Figure 6.16). Therefore, we have existence of a positive fixed point (limit cycle) for $\beta > 0$ if $\sigma_0 < 0$ and for

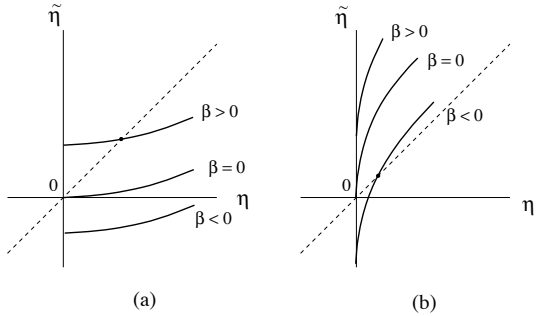


FIGURE 6.16. Fixed points of the Poincaré map: (a) $\sigma_0 < 0$; (b) $\sigma_0 > 0$.

$\beta < 0$ if $\sigma_0 > 0$. Stability and uniqueness of the cycle also simply follow from analysis of the map. □

**Remark:**

Until now we have considered only so-called "small" homoclinic orbits in this section. There is another type of homoclinic orbits, namely, "big" homoclinic orbits corresponding to the different return direction. All the

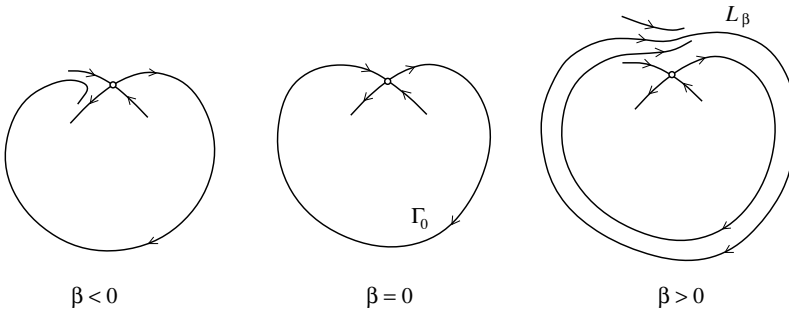


FIGURE 6.17. Bifurcation of a "big" saddle homoclinic orbit.

results obtained are valid for them as well (see Figure 6.17, where a bifurcation diagram for the case $\sigma_0 < 0$ is presented). ♢

**Example 6.1 (Explicit homoclinic bifurcation)** Consider the following system due to Sandstede [1997*a*]:

$$\begin{cases} \dot{x} &= -x + 2y + x^2, \\ \dot{y} &= (2-\alpha)x - y - 3x^2 + \frac{3}{2}xy, \end{cases} \tag{6.8}$$

where $\alpha$ is a parameter.

The origin $(x, y) = (0, 0)$ is a saddle for all sufficiently small $|\alpha|$. At $\alpha = 0$, this saddle has eigenvalues

$$\lambda_1 = 1, \quad \lambda_2 = -3,$$

with $\sigma_0 = -2 < 0$. Moreover, at this parameter value, there exists a homoclinic orbit to the origin (see Figure 6.18). Indeed, the *Cartesian leaf*,

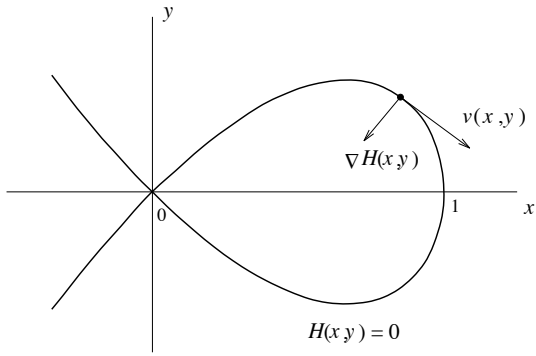


FIGURE 6.18. The homoclinic orbit of (6.8) at $\alpha = 0$.

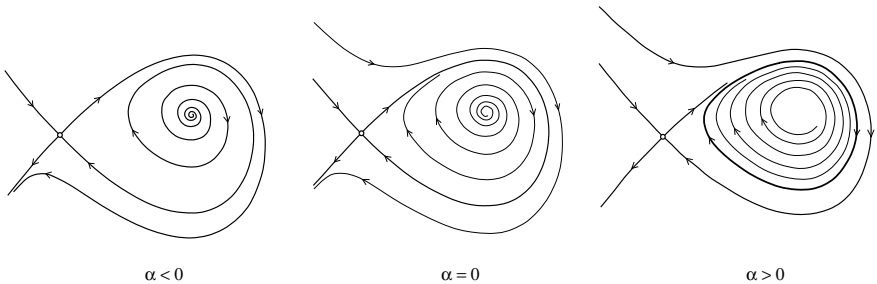


FIGURE 6.19. Homoclinic bifurcation in (6.8): A stable limit cycle exists for small $\alpha > 0$.

$$H(x, y) \equiv x^2(1 - x) - y^2 = 0,$$

consists of orbits of (6.8) for $\alpha = 0$. One of these orbits is homoclinic to the saddle $0 = (0, 0)$. To verify this fact, we have to prove that the vector field defined by (6.8) with $\alpha = 0$,

$$v(x, y) = \left(-x + 2y + x^2, 2x - y - 3x^2 + \frac{3}{2}xy\right)^T,$$

is tangent to the curve $H(x, y) = 0$ at all nonequilibrium points. Equivalently, it is sufficient to check that $v$ is orthogonal along the curve to the *normal vector* to the curve. A normal vector is given by the gradient of the function $H$:

$$(\nabla H)(x, y) = (2x - 3x^2, -2y)^T.$$

Then, a direct calculation shows that

$$\langle v, \nabla H \rangle = 0$$

along the curve $H = 0$ (check!).

Thus, system (6.8) has an algebraic homoclinic orbit at $\alpha = 0$ with $\sigma_0 < 0$. One can prove that the transversality condition $\beta' \neq 0$ also holds at $\alpha = 0$ (see Exercise 13). Therefore, Theorem 6.1 is applicable, and a unique and stable limit cycle bifurcates from the homoclinic orbit under small variation of $\alpha$ (see Figure 6.19). $\diamond$

**Example 6.2 (Homoclinic bifurcation in a slow-fast system)** Consider the following system

$$\begin{cases} \dot{x} &= 1 + x - y - x^2 - x^3, \\ \dot{y} &= \varepsilon \left[ -1 + (1 - 4\alpha)x + 4xy \right], \end{cases} \tag{6.9}$$

where $\alpha$ is a "control" parameter and $0 < \varepsilon \ll 1$. We shall show that the system undergoes a homoclinic bifurcation at some value of $\alpha$ close to zero. More precisely, there is a continuous function $\alpha_0 = \alpha_0(\varepsilon)$ defined for sufficiently small $\varepsilon \geq 0$, $\alpha_0(0) = 0$ such that the system has a homoclinic orbit to a saddle at $\alpha = \alpha_0(\varepsilon)$. Moreover, the genericity conditions of the Andronov-Leontovich theorem are satisfied, and a unique and stable limit cycle bifurcates from the homoclinic orbit under the variation of $\alpha$ for $\alpha < \alpha_0$.

The nontrivial zero-isoclines of (6.9) are graphs of the following functions:

$$\dot{x} = 0 : \; y = (x + 1)(1 - x^2)$$

and

$$\dot{y} = 0 : \; y = \frac{1 - x}{4x} + \alpha;$$

their shape at $\alpha = 0$ is presented in Figure 6.20.

If $\alpha = 0$, the system has a saddle equilibrium point $E_0 : (x, y) = (1, 0)$ for all $\varepsilon > 0$. It can easily be checked that *near* the saddle $E_0$ the stable invariant manifold $W^s(E_0)$ approaches the $x$-axis while the unstable manifold $W^u(E_0)$ tends to the zero-isocline $\dot{x} = 0$, as $\varepsilon \to 0$. The global behavior of the upper branch $W_1^u$ of the unstable manifold as $\varepsilon \to 0$ is also clear. It approaches a *singular* orbit composed of two *slow* motions along the isocline $\dot{x} = 0$ ($E_0A$ and $BC$) and two *fast* jumps in the horizontal direction ($AB$ and $CE_0$; the latter happens along the $x$-axis) (see Figure 6.20). This singular orbit returns to $E_0$, thus forming a *singular homoclinic orbit*.

This construction can be carried out for all sufficiently small $\alpha \neq 0$ (see Figure 6.21). The equilibrium point will shift away from the $x$-axis and will have the $y$-coordinate equal to $\alpha$. Despite this, a singular orbit to which $W_1^u$ tends as $\varepsilon \to 0$ still arrives at a neighborhood of the saddle along

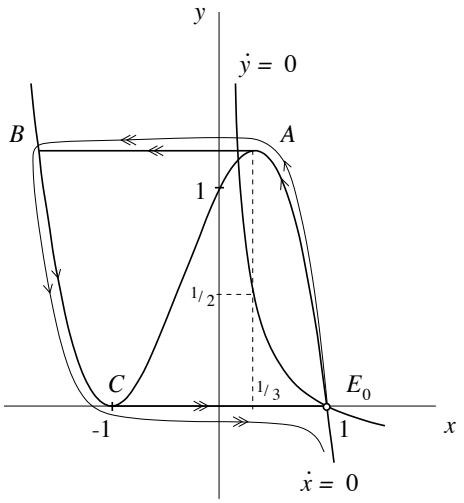


FIGURE 6.20. Zero-isoclines of (6.9) and the corresponding singular homoclinic orbit.

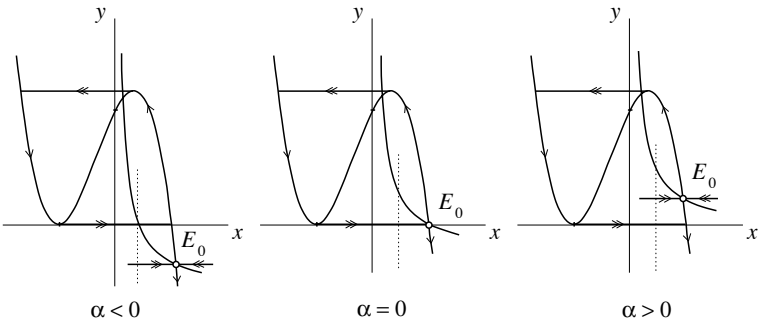


FIGURE 6.21. Singular homoclinic bifurcation in (6.9).

the $x$-axis. Therefore, there is a *singular split function* $\beta_0(\alpha)$ measured along a vertical cross-section near the saddle which equals $\alpha$ : $\beta_0(\alpha) = \alpha$. Obviously, $\beta_0'(0) > 0$. Meanwhile, the singular orbit tends to a *singular limit cycle* if $\alpha < 0$.

Thus, we have a generic *singular homoclinic bifurcation* at $\alpha = 0$ in the singular limit $\varepsilon = 0$. This implies the existence of a generic homoclinic bifurcation at $\alpha = \alpha_0(\varepsilon)$ for sufficiently small $\varepsilon > 0$. One can show this using nonstandard analysis. To prove it in a standard way, one has to check that the split function $\beta(\alpha, \varepsilon)$ can be represented for all sufficiently small $\varepsilon > 0$ as

$$\beta(\alpha, \varepsilon) = \beta_0(\alpha) + \varphi(\alpha, \varepsilon),$$

where $\varphi(\alpha, \varepsilon)$ (considered as a function of $\alpha$ for small $|\alpha|$) vanishes uniformly with its first derivative as $\varepsilon \to 0$. Then, elementary arguments[4] show the existence of a unique continuous function $\alpha_0(\varepsilon)$, $\alpha_0(0) = 0$, such that

$$\beta(\alpha_0(\varepsilon), \varepsilon) = 0$$

for all sufficiently small $\varepsilon \geq 0$. Actually, $\alpha_0(\varepsilon)$ is smooth for $\varepsilon > 0$. Therefore, the system has a homoclinic orbit at $\alpha = \alpha_0(\varepsilon)$ for all sufficiently small $\varepsilon$. The corresponding saddle quantity $\sigma_0$ is negative and $\beta_\alpha(\alpha_0(\varepsilon), \varepsilon) \neq 0$, thus, Theorem 6.1 is applicable to (6.9). $\diamond$

**More remarks on Theorem 6.1:**

(1) Condition (H.2) of Theorem 6.1 is equivalent to the transversality of the intersection of certain invariant manifolds of the *extended* system

$$\begin{cases} \dot{x} &= f(x, \alpha), \\ \dot{\alpha} &= 0. \end{cases} \tag{6.10}$$

Let $x_0(\alpha)$ denote a one-parameter family of the saddles in (6.4) for small $|\alpha|$. This family defines an invariant set of (6.10) – a curve of equilibria. This curve has two-dimensional unstable and stable manifolds, $\mathcal{W}^u$ and $\mathcal{W}^s$, whose slices $\alpha = \text{const}$ coincide with the corresponding one-dimensional unstable and stable manifolds $W^u$ and $W^s$ of the saddle $x_0(\alpha)$ in (6.4) (see Figure 6.22). Condition (H.2) (meaning that $W^u$ and $W^s$ split with nonzero

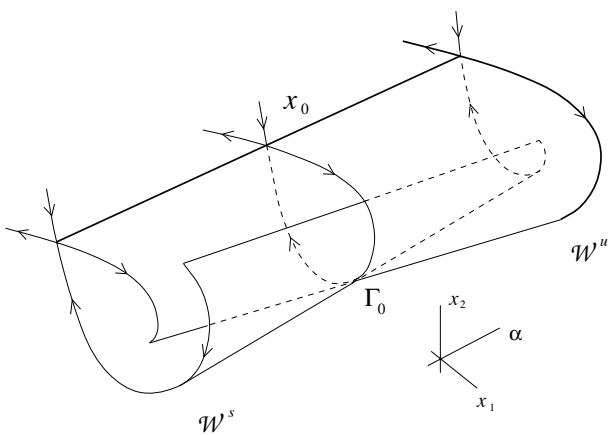


FIGURE 6.22. Transversal intersection of invariant manifolds $\mathcal{W}^u$ and $\mathcal{W}^s$.

velocity as $\alpha$ crosses $\alpha = 0$) translates exactly to the transversality of the intersection of $\mathcal{W}^u$ and $\mathcal{W}^s$ along $\Gamma_0$ at $\alpha = 0$ in the three-dimensional

[4]The only difficulty that should be overcome is that $\varphi(\alpha, \varepsilon)$ is not differentiable with respect to $\varepsilon$ at $\varepsilon = 0$ (see Exercise 8).

state space of (6.10). In Section 6.4.1 we will show that the transversality is equivalent to the *Melnikov condition*:

$$\int_{-\infty}^{+\infty} \exp\left[-\int_0^t \left(\frac{\partial f_1}{\partial x_1}+\frac{\partial f_2}{\partial x_2}\right) d\tau\right] \left(f_1\frac{\partial f_2}{\partial \alpha}-f_2\frac{\partial f_1}{\partial \alpha}\right) dt \neq 0,$$

where all expressions involving $f=(f_1,f_2)^T$ are evaluated at $\alpha=0$ along a solution $x^0(\cdot)$ of (6.4) corresponding to the homoclinic orbit $\Gamma_0$.

(2) One can construct a *topological normal form* for the homoclinic bifurcation on the plane. Consider the $(\xi,\eta)$-plane and introduce two domains:

the unit square

$$\Omega_0=\{(\xi,\eta):\ |\xi|\le 1,\ |\eta|\le 1\}$$

and the rectangle

$$\Omega_1=\{(\xi,\eta):\ 1\le \xi\le 2,\ |\eta|\le 1\}$$

(see Figure 6.23). Define a two-dimensional manifold $\Omega$ by glueing $\Omega_0$ and

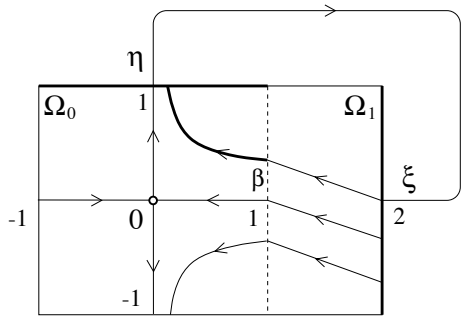


FIGURE 6.23. Topological normal form for homoclinic bifurcation.

$\Omega_1$ along the vertical segment $\{\xi=1,\ |\eta|\le 1\}$ and identifying the upper boundary of $\Omega_0$ with the right boundary of $\Omega_1$ (i.e., glueing points $(\xi,1)$ and $(2,\xi)$ for $|\xi|\le 0$). The resulting manifold is homeomorphic to a simple band.

Consider a system of ODEs in $\Omega$ that is defined by

$$\left\{\begin{array}{rcl}\dot\xi &=& \lambda_1(\alpha)\xi,\\ \dot\eta &=& \lambda_2(\alpha)\eta,\end{array}\right. \tag{6.11}$$

in $\Omega_0$ and by

$$\left\{\begin{array}{rcl}\dot\xi &=& -1,\\ \dot\eta &=& \beta(\alpha)\eta,\end{array}\right. \tag{6.12}$$

in $\Omega_1$, where $\lambda_{1,2}$ and $\beta$ are smooth functions of a parameter $\alpha$. The behavior of thus defined piecewise-smooth system in $\Omega$ is similar to that of

(6.4) near the homoclinic orbit (cf. Figures 6.15 and 6.23). If $\lambda_1 < 0 < \lambda_2$, the constructed system has a saddle at the origin. At $\beta = 0$ this saddle has a homoclinic orbit $\tilde{\Gamma}_0$ composed by two segments of the coordinate axes: $\{\xi = 0,\ 0 < \eta \le 1\}$ and $\{\eta = 0,\ 0 < \xi \le 2\}$. For small $\beta \neq 0$ this homoclinic orbit breaks down, with the parameter $\beta$ playing the role of the split function. Provided the saddle quantity $\sigma_0 = \lambda_1(0) + \lambda_2(0) \neq 0$, a unique limit cycle bifurcates from $\tilde{\Gamma}_0$. This can be seen from the Poincaré map defined by the system (6.11), (6.12) in the cross-section $\{\xi = 1,\ 0 \le \eta \le 1\}$:

$$\eta \mapsto \beta + \eta^{-\frac{\lambda_1}{\lambda_2}}.$$

Actually, the following theorem holds.

**Theorem 6.2** *Under the assumptions of Theorem* 6.1*, the system* (6.4) *is locally topologically equivalent near the homoclinic orbit* $\Gamma_0$ *for nearby parameter values to the system defined by* (6.11) *and* (6.12) *in* $\Omega$ *near* $\tilde{\Gamma}_0$ *for small* $|\beta|$*. Moreover, all such systems with* $\sigma_0 < 0$ $(\sigma_0 > 0)$ *are locally topologically equivalent near the respective homoclinic orbits for nearby parameter values.* □

The last statement of the theorem follows from the fact that, for $\sigma_0 < 0$, the constructed system in $\Omega$ is locally topologically equivalent near $\tilde{\Gamma}_0$ for small $|\beta|$ to this system with constant $\lambda_1 = -2,\ \lambda_2 = 1$, while, for $\sigma_0 > 0$, it is equivalent to that with $\lambda_1 = -1, \lambda_2 = 2$. ♢

## 6.3 Homoclinic bifurcations in three-dimensional systems: Shil'nikov theorems

A three-dimensional state space gives rise to a wider variety of homoclinic bifurcations, some of which involve an *infinite number* of periodic orbits. As is known from Chapter 3, the two simplest types of hyperbolic equilibria in $\mathbb{R}^3$ allowing for homoclinic orbits are *saddles* and *saddle-foci*. We assume from now on that these points have a one-dimensional unstable manifold $W^u$ and a two-dimensional stable manifold $W^s$ (otherwise, reverse the time direction). In the saddle case, we assume that the eigenvalues of the equilibrium are simple and satisfy the inequalities $\lambda_1 > 0 > \lambda_2 > \lambda_3$. Then, as we have seen in Chapter 2, all the orbits on $W^s$ approach the equilibrium along a one-dimensional eigenspace of the Jacobian matrix corresponding to $\lambda_2$ except two orbits approaching the saddle along an eigenspace corresponding to $\lambda_3$ (see Figure 2.4(a)).

**Definition 6.6** *The eigenvalues with negative real part that are closest to the imaginary axis are called* leading (*or* principal) *eigenvalues, while the corresponding eigenspace is called a* leading (*or* principal) *eigenspace.*

Thus, almost all orbits on $W^s$ approach a generic saddle along the one-dimensional leading eigenspace. In the saddle-focus case, there are *two* leading eigenvalues $\lambda_2 = \bar{\lambda}_3$, and the leading eigenspace is two-dimensional (see Figure 2.4(b)).

**Definition 6.7** *A* saddle quantity $\sigma$ *of a saddle* (*saddle-focus*) *is the sum of the positive eigenvalue and the real part of a leading eigenvalue.*

Therefore, $\sigma = \lambda_1 + \lambda_2$ for a saddle, and $\sigma = \lambda_1 + \text{Re } \lambda_{2,3}$ for a saddle-focus.

The table below briefly presents some general results Shil'nikov obtained concerning the number and stability of limit cycles generated via homoclinic bifurcations in $\mathbb{R}^3$. The column entries specify the type of the equilibrium having a homoclinic orbit, while the row entries give the possible sign of the corresponding saddle quantity.

| | *Saddle* | *Saddle-focus* |
|---|---|---|
| $\sigma_0 < 0$ | one stable cycle | one stable cycle |
| $\sigma_0 > 0$ | one saddle cycle | $\infty$ saddle cycles |

The following theorems give more precise information.

**Theorem 6.3 (Saddle, $\sigma_0 < 0$)** *Consider a three-dimensional system*

$$\dot{x} = f(x, \alpha), \quad x \in \mathbb{R}^3, \ \alpha \in \mathbb{R}^1, \tag{6.13}$$

*with smooth $f$, having at $\alpha = 0$ a saddle equilibrium point $x_0 = 0$ with real eigenvalues $\lambda_1(0) > 0 > \lambda_2(0) \geq \lambda_3(0)$ and a homoclinic orbit $\Gamma_0$. Assume the following genericity conditions hold:*

(H.1) $\sigma_0 = \lambda_1(0) + \lambda_2(0) < 0$;
(H.2) $\lambda_2(0) \neq \lambda_3(0)$;
(H.3) $\Gamma_0$ *returns to* $x_0$ *along the leading eigenspace*;
(H.4) $\beta'(0) \neq 0$, *where* $\beta(\alpha)$ *is the split function defined earlier.*

*Then, the system* (6.13) *has a unique and stable limit cycle $L_\beta$ in a neighborhood $U_0$ of $\Gamma_0 \cup x_0$ for all sufficiently small $\beta > 0$. Moreover, all such systems are locally topologically equivalent near $\Gamma_0 \cup x_0$ for small $|\alpha|$.* □

The theorem is illustrated in Figure 6.24. The unstable manifold $W^u(x_0)$ tends to the cycle $L_\beta$. The period of the cycle tends to infinity as $\beta$ approaches zero. The (nontrivial) multipliers of the cycle are positive and inside the unit circle: $|\mu_{1,2}| < 1$. There are no periodic orbits of (6.13) in $U_0$ for all sufficiently small $\beta \leq 0$. Thus, the bifurcation is completely analogous to that in the planar case. The proof of the theorem will be sketched later (see also Exercise 10).

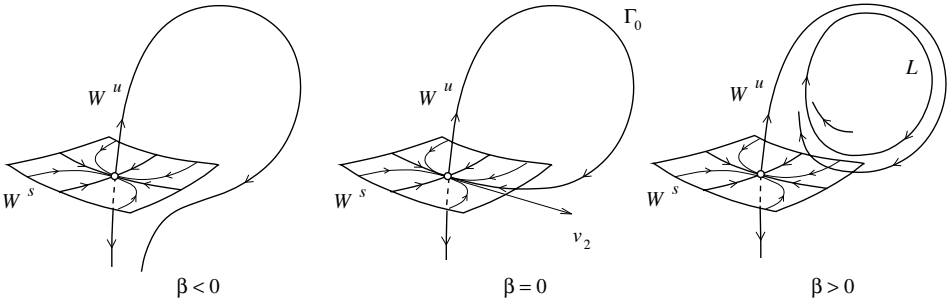


FIGURE 6.24. Saddle homoclinic bifurcation with $\sigma_0 < 0$.

**Theorem 6.4 (Saddle-focus, $\sigma_0 < 0$)** *Suppose that a three-dimensional system*

$$\dot{x} = f(x, \alpha), \quad x \in \mathbb{R}^3, \ \alpha \in \mathbb{R}^1, \tag{6.14}$$

*with a smooth $f$, has at $\alpha = 0$ a saddle-focus equilibrium point $x_0 = 0$ with eigenvalues $\lambda_1(0) > 0 > \operatorname{Re} \lambda_{2,3}(0)$ and a homoclinic orbit $\Gamma_0$. Assume the following genericity conditions hold:*

(H.1) $\sigma_0 = \lambda_1(0) + \operatorname{Re} \lambda_{2,3}(0) < 0$;
(H.2) $\lambda_2(0) \neq \lambda_3(0)$;
(H.3) $\beta'(0) \neq 0$, *where $\beta(\alpha)$ is the split function.*

*Then, system* (6.14) *has a unique and stable limit cycle $L_\beta$ in a neighborhood $U_0$ of $\Gamma_0 \cup x_0$ for all sufficiently small $\beta > 0$, as presented in* Figure 6.25. □

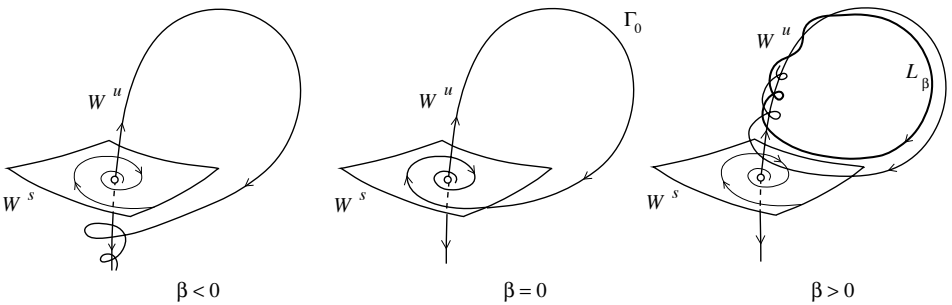


FIGURE 6.25. Saddle-focus homoclinic bifurcation with $\sigma_0 < 0$.

There are no periodic orbits of (6.14) in $U_0$ for all sufficiently small $\beta \leq 0$. The unstable manifold $W^u(x_0)$ tends to the cycle $L_\beta$. The cycle period tends to infinity as $\beta$ approaches zero. The (nontrivial) multipliers of the cycle are complex, $\mu_2 = \bar{\mu_1}$, and lie inside the unit circle: $|\mu_{1,2}| < 1$.

The analogy with the planar case, however, terminates here. We cannot say that the bifurcation diagrams of all systems (6.10) satisfying (H.1)–(H.3) are topologically equivalent. As a rule, they are *nonequivalent* since

the real number

$$\nu_0 = -\frac{\lambda_1(0)}{\text{Re } \lambda_{2,3}(0)} \tag{6.15}$$

is a topological invariant for systems with a homoclinic orbit to a saddle-focus. The nature of this invariant will be clearer later. Thus, although there is a unique limit cycle for $\beta > 0$ in all such systems, the exact topology of their phase portraits can differ. Fortunately, this is not very important in most applications.

Before treating the saddle case with $\sigma_0 > 0$, we have to look at the topology of the invariant manifold $W^s(x_0)$ near $\Gamma_0$ more closely. Suppose we have a three-dimensional system with a saddle equilibrium point $x_0$ having simple eigenvalues and a homoclinic orbit returning along the leading eigenspace to this saddle. Let us fix a small neighborhood $U_0$ of $\Gamma_0 \cap x_0$. The homoclinic orbit $\Gamma_0$ belongs to the stable manifold $W^s(x_0)$ entirely. Therefore, the manifold $W^s(x_0)$ can be extended "back in time" along $\Gamma_0$

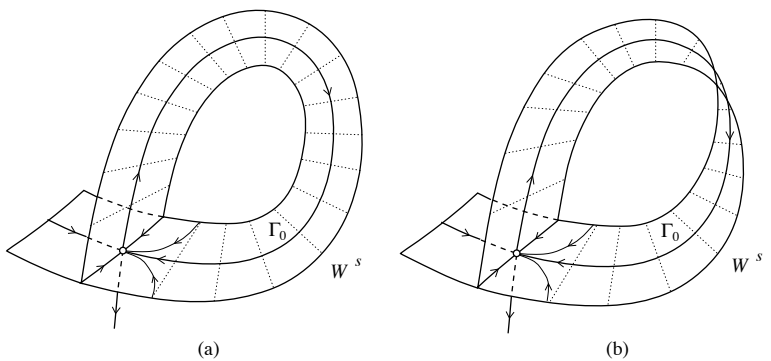


FIGURE 6.26. (a) Simple and (b) twisted stable manifolds near a homoclinic orbit to a saddle.

within the fixed neighborhood. At each point $\varphi^t x \in \Gamma_0$, a *tangent plane* to this manifold is well defined. For $t \to +\infty$, this plane is spanned by the stable eigenvectors $v_2$ and $v_3$. Generically, it approaches the plane spanned by the unstable eigenvector $v_1$ and the nonleading eigenvector $v_3$, as $t \to -\infty$. Thus, generically the manifold $W^s(x_0)$ intersects itself near the saddle along the two exceptional orbits on $W^s(x_0)$ that approach the saddle along the nonleading eigenspace[5] (see Figure 6.26). Therefore, the part of $W^s(x_0)$ in $U_0$ to which belongs the homoclinic orbit $\Gamma_0$ is (generically) a two-dimensional nonsmooth submanifold $\mathcal{M}$. As is well known from

[5]This property (often called the *strong inclination property*) was first established by Shil'nikov and is discussed in Exercise 9. See also Chapter 10, where we describe how to verify this property numerically.

elementary topology, such a manifold is topologically equivalent to either a *simple* or a *twisted* band. The latter is known as the *Möbius band*.

**Definition 6.8** *If $\mathcal{M}$ is topologically equivalent to a simple band, the homoclinic orbit $\Gamma_0$ is called* simple (*or* nontwisted). *If $\mathcal{M}$ is topologically equivalent to a Möbius band, the homoclinic orbit is called* twisted.

We are now ready to formulate the relevant theorem.

**Theorem 6.5 (Saddle, $\sigma_0 > 0$)** *Consider a three-dimensional system*

$$\dot{x} = f(x, \alpha), \quad x \in \mathbb{R}^3, \ \alpha \in \mathbb{R}^1, \tag{6.16}$$

*with smooth $f$, having at $\alpha = 0$ a saddle equilibrium point $x_0 = 0$ with real eigenvalues $\lambda_1(0) > 0 > \lambda_2(0) \geq \lambda_3(0)$ and a homoclinic orbit $\Gamma_0$. Assume that the following genericity conditions hold:*

(H.1) $\sigma_0 = \lambda_1(0) + \lambda_2(0) > 0$;
(H.2) $\lambda_2(0) \neq \lambda_3(0)$;
(H.3) $\Gamma_0$ *returns to $x_0$ along the leading eigenspace*;
(H.4) $\Gamma_0$ *is simple or twisted*;
(H.5) $\beta'(0) \neq 0$, *where $\beta(\alpha)$ is the split function.*

*Then, for all sufficiently small $|\alpha|$, there exists a neighborhood $U_0$ of $\Gamma_0 \cap x_0$ in which a unique saddle limit cycle $L_\beta$ bifurcates from $\Gamma_0$. The cycle exists for $\beta < 0$ if $\Gamma_0$ is nontwisted, and for $\beta > 0$ if $\Gamma_0$ is twisted. Moreover, all such systems* (6.16) *with simple* (*twisted*) $\Gamma_0$ *are locally topologically equivalent in a neighborhood $U_0$ of $\Gamma_0 \cap x_0$ for sufficiently small $|\alpha|$.* □

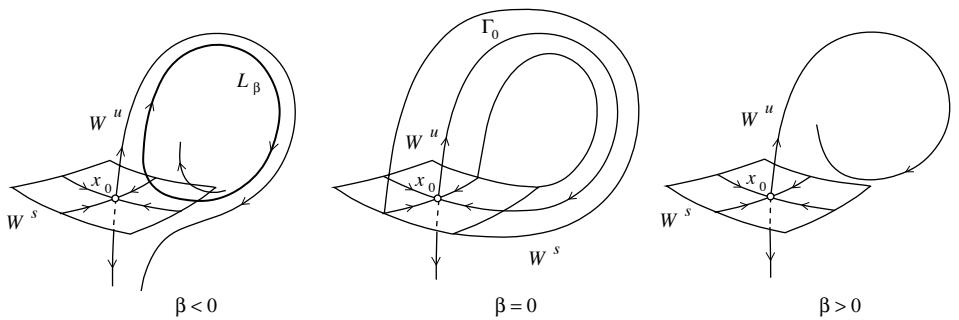


FIGURE 6.27. Simple saddle homoclinic bifurcation with $\sigma_0 > 0$.

The bifurcation diagrams to both cases are presented in Figures 6.27 and 6.28, respectively. In both (simple and twisted) cases a unique saddle limit cycle $L_\beta$ bifurcates from the homoclinic orbit. Its period tends to infinity as $\beta$ approaches zero. Remarkably, the direction of the bifurcation is determined by the topology of $\mathcal{M}$.

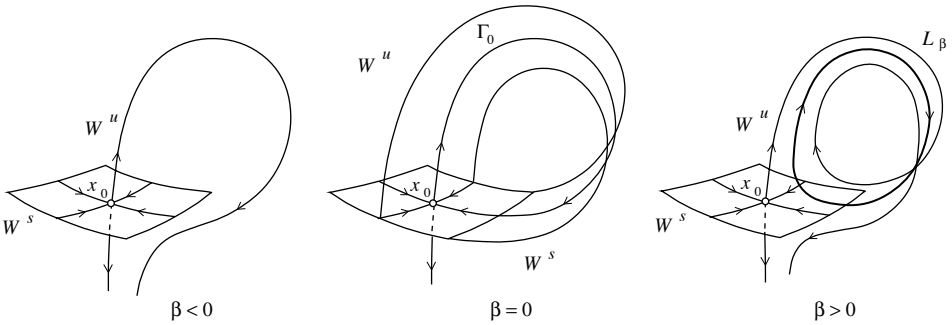


FIGURE 6.28. Twisted saddle homoclinic bifurcation with $\sigma_0 > 0$.

If the homoclinic orbit is simple, there is a saddle cycle $L_\beta$ for $\beta < 0$. Its multipliers are positive: $\mu_1 > 1 > \mu_2 > 0$. The stable and unstable manifolds $W^{s,u}(L_\beta)$ of the cycle are (locally) simple bands.

If the homoclinic orbit is twisted, there is a saddle cycle $L_\beta$ for $\beta > 0$. Its multipliers are negative: $\mu_1 < -1 < \mu_2 < 0$. The stable and unstable manifolds $W^{s,u}(L_\beta)$ of the cycle are (locally) Möbius bands.

**Sketch of the proof of Theorems 6.2 and 6.4:**

We outline the proof of the theorems in the saddle cases. There are coordinates in $\mathbb{R}^3$ in which the manifolds $W^s(x_0)$ and $W^u(x_0)$ are linear in some neighborhood of $x_0$. Suppose system (6.13) (or (6.16)) is already written in these coordinates and, moreover, locally: $W^s(x_0) \subset \{x_1 = 0\}$, $W^u(x_0) \subset \{x_2 = x_3 = 0\}$. Let the $x_2$-axis be the leading eigenspace and the $x_3$-axis be the nonleading eigenspace. Introduce a rectangular two-dimensional cross-section $\Sigma \subset \{x_2 = \varepsilon_2\}$ and an auxiliary rectangular cross-section $\Pi \subset \{x_1 = \varepsilon_1\}$, where $\varepsilon_{1,2}$ are small enough. Assume that $\Gamma_0$ intersects both local cross-sections (see Figure 6.29). As in the planar case, define a Poincaré map $P : \Sigma^+ \to \Sigma$ along the orbits of (6.13), mapping the upper part $\Sigma^+$ of $\Sigma$ corresponding to $x_1 \geq 0$ into $\Sigma$. Represent $P$ as a superposition

$$P = Q \circ \Delta,$$

where $\Delta : \Sigma^+ \to \Pi$ is a near-to-saddle map, and $Q : \Pi \to \Sigma$ is a map along the global part of $\Gamma_0$. The construction can be carried out for all sufficiently small $|\beta|$.

The local map $\Delta$ is "essentially"[6] defined by the linear part of (6.13) near the saddle. It can be seen that the image of $\Sigma^+$ under the action of map $\Delta$, $\Delta\Sigma^+$, looks like a "horn" with a cusp on the $x_1$-axis (on $\Gamma_0$, in other words). Actually, the cross-sections $\Sigma$ and $\Pi$ should be chosen in such a way that $\Delta\Sigma^+ \subset \Pi$. The global map $Q$ maps this "horn" back into the

[6]Unfortunately, there are obstacles to $C^k$-linearization with $k \geq 1$ in this case. For example, $C^1$-linearization is impossible if $\lambda_2 = \lambda_1 + \lambda_3$ (see Appendix 2).

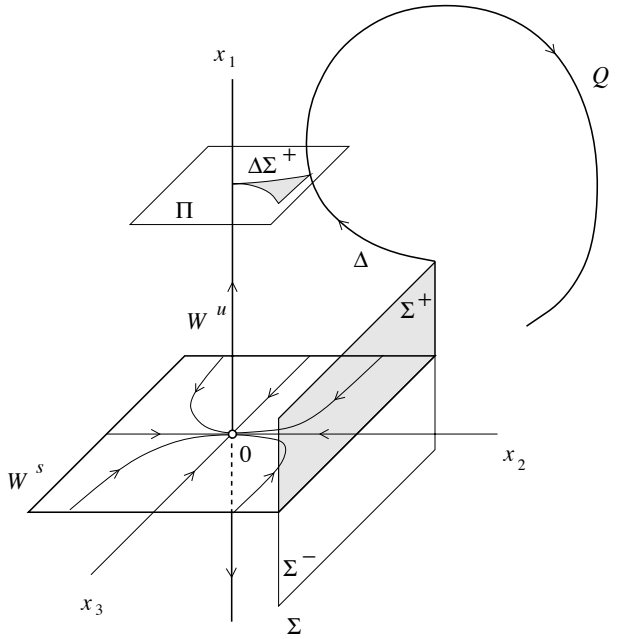


FIGURE 6.29. Construction of the Poincaré map in the saddle case.

plane $\{x_2 = \varepsilon_2\}$. If $\Gamma_0$ is simple, $P\Sigma^+$ intersects nontrivially with $\Sigma^+$ at $\beta = 0$; otherwise, the intersection with $\Sigma^- \equiv \Sigma \setminus \Sigma^+$ is nontrivial (see Figure 6.29). Note that the transversality of the "horn" to the intersection of $W^s(x_0)$ with $\Sigma$ follows from the orientability or nonorientability of the manifold $\mathcal{M}$.

According to the sign of the saddle quantity $\sigma_0$ and the twisting of the homoclinic orbit, there are several cases of relative position of $P\Sigma^+$ with respect to $\Sigma$ (Figures 6.30 and 6.31). A close look at these figures, actually, completes the proof. If $\sigma_0 < 0$ (Theorem 6.2, Figure 6.29), the map $P$ is a contraction in $\Sigma^+$ for $\beta > 0$ and thus has a unique and stable fixed point in $P\Sigma^+$ corresponding to a stable limit cycle. If $\sigma_0 > 0$ (Theorem 6.4, Figure 6.30), the map $P$ contracts along the $x_3$-axis and expands along the "horn." Therefore it has a saddle fixed point in $P\Sigma^+$ for $\beta < 0$ or $\beta > 0$, depending on the twisting of the homoclinic orbit. □

**Remark:**

Because the map $P$ always acts as a contraction along the $x_3$-axis, the fixed-point analysis reduces (see Exercise 10) to the analysis of a one-dimensional map having the form

$$x_1 \mapsto \beta + A x_1^{-\frac{\lambda_1}{\lambda_2}} + \cdots$$

that is similar to that in the Andronov-Leontovich theorem but $A$ can be either positive (simple homoclinic orbit) or negative (twisted homoclinic

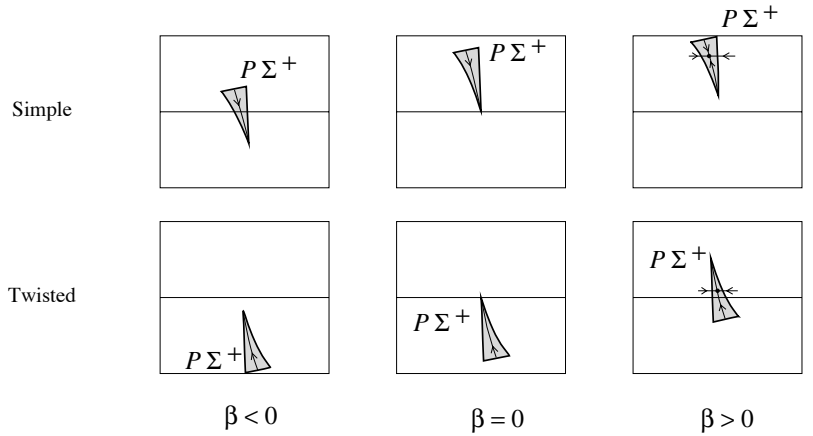


FIGURE 6.30. The relative position of $P\Sigma^+$ with respect to $\Sigma$ in the case $\sigma_0 < 0$.

orbit).

Actually, this analogy can be extended further, since in this case there is a two-dimensional attracting invariant "center manifold" near the homoclinic orbit (see Section 6.4). ♢

The last case is the most difficult.

**Theorem 6.6 (Saddle-focus, $\sigma_0 > 0$)** *Suppose that a three-dimensional system*

$$\dot{x} = f(x, \alpha), \quad x \in \mathbb{R}^3, \ \alpha \in \mathbb{R}^1, \tag{6.17}$$

*with a smooth $f$, has at $\alpha = 0$ a saddle-focus equilibrium point $x_0 = 0$ with eigenvalues $\lambda_1(0) > 0 > \mathrm{Re}\ \lambda_{2,3}(0)$ and a homoclinic orbit $\Gamma_0$. Assume that the following genericity conditions hold:*

(H.1) $\sigma_0 = \lambda_1(0) + \mathrm{Re}\ \lambda_{2,3}(0) > 0$;
(H.2) $\lambda_2(0) \neq \lambda_3(0)$.

*Then, system* (6.17) *has an infinite number of saddle limit cycles in a neighborhood $U_0$ of $\Gamma_0 \cup x_0$ for all sufficiently small $|\beta|$.* □

**Sketch of the proof of Theorems 6.3 and 6.5:**

To outline the proof, select a coordinate system in which $W^s(x_0)$ is (locally) the plane $x_1 = 0$, while $W^u(x_0)$ is (also locally) the line $x_2 = x_3 = 0$ (see Figure 6.32). Introduce two-dimensional cross-sections $\Sigma$ and $\Pi$, and represent the Poincaré map $P : \Sigma^+ \to \Sigma$ as a superposition $P = Q \circ \Delta$ of two maps: a near-to-saddle $\Delta : \Sigma^+ \to \Pi$ and a global $Q : \Pi \to \Sigma$, as in the proof of Theorems 6.2 and 6.4.[7]

[7]Actually, in the case of the saddle-focus, there is a $C^1$ change of coordinates that locally linearizes the system (see Appendix 2). It allows one to compute $\Delta$ analytically.

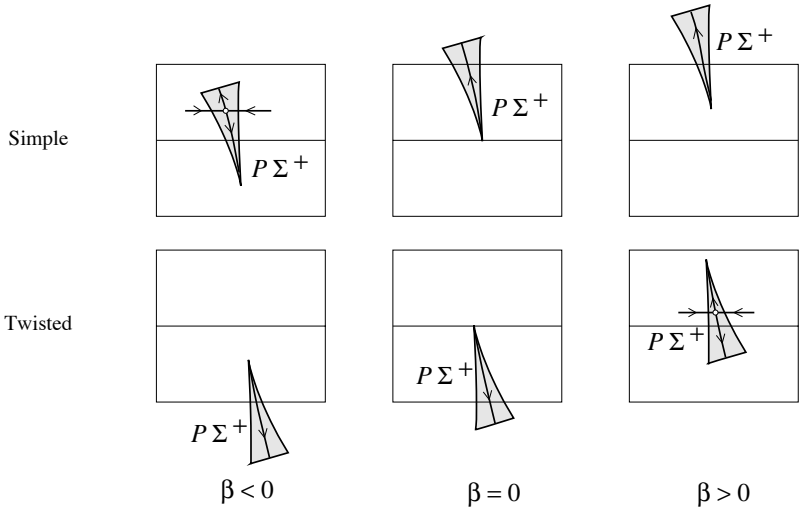


FIGURE 6.31. Relative position of $P\Sigma^+$ with respect to $\Sigma$ in the case $\sigma_0 > 0$.

The image $\Delta\Sigma^+$ of $\Sigma^+$ on $\Pi$ is no longer a horn but a "solid spiral" (sometimes called a *Shil'nikov snake*). The global map $Q$ maps the "snake" to the plane containing $\Sigma$.

Assume, first, that $\beta = 0$ and consider the intersection of the "snake" image (i.e., $P\Sigma^+$) with the local cross-section $\Sigma$. The origin of the "snake" is at the intersection of $\Gamma_0$ with $\Sigma$. The intersection of $\Sigma$ with $W^s(x_0)$ splits the "snake" into an infinite number of *upper* and *lower* "half-spirals." The preimages $\Sigma_i$ of the upper "half-spirals" $P\Sigma_i$, $i = 1, 2, \ldots$, are horizontal strips in $\Sigma^+$ (see Figure 6.33). If the saddle quantity $\sigma_0 > 0$, the intersection $\Sigma_i \cap P\Sigma_i$ is nonempty and consists of two components for $i \geq i_0$, where $i_0$ is some positive number ($i_0 = 2$ in Figure 6.33(a)). Each of these intersections forms a Smale horseshoe (see Chapter 1). It can be checked that the necessary expansion conditions are satisfied. Thus, each horseshoe gives an infinite number of saddle fixed points. These fixed points correspond to saddle limit cycles of (6.17). If $\sigma_0 < 0$, there is some $i_0 > 0$ such that for $i \geq i_0$ the intersection $\Sigma_i \cap P\Sigma_i$ is empty ($i_0 = 2$ in Figure 6.33(b)). Thus, there are no fixed points of $P$ in $\Sigma^+$ close to $\Gamma_0$.

If $\beta \neq 0$, the point corresponding to $\Gamma_0$ is displaced from the horizontal line in $\Sigma$. Therefore, if $\sigma_0 > 0$, there remains only a *finite* number of Smale horseshoes. They still give an infinite number of saddle limit cycles in (6.17) for all sufficiently small $|\beta|$. In the case $\sigma_0 < 0$, the map $P$ is a contraction in $\Sigma^+$ for $\beta > 0$ and thus has a unique attracting fixed point corresponding to a stable limit cycle of (6.14). There are no periodic orbits if $\beta < 0$. □

**Remarks:**

(1) As in the saddle-focus case with $\sigma_0 < 0$, it cannot be said that the bifurcation diagrams of all systems (6.15) satisfying (H.1)–(H.2) are topo-

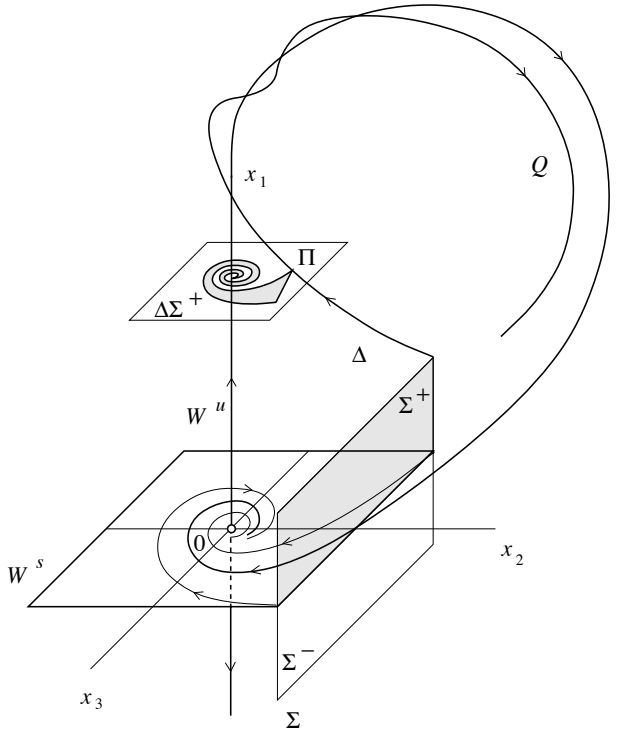


FIGURE 6.32. Construction of the Poincaré map in the saddle-focus case.

logically equivalent. The reason is the same: the topological invariance of $\nu_0$ given by (6.15). Actually, the complete topological structure of the phase portrait near the homoclinic orbit is not known, although some substantial information is available due to Shil'nikov. Let $\tilde{\Omega}(\nu)$ be the set of all nonequivalent bi-infinite sequences

$$\omega = \{\ldots, \omega_{-2}, \omega_{-1}, \omega_0, \omega_1, \omega_2, \ldots\},$$

where $\omega_i$ are nonnegative integers such that

$$\omega_{i+1} < \nu\omega_i$$

for all $i = 0, \pm 1, \pm 2, \ldots$, and for some real number $\nu > 0$. Then, at $\beta = 0$ there is a subset of orbits of (6.17) located in a neighborhood $U_0$ of $\Gamma_0 \cup x_0$ for all $t \in \mathbb{R}^1$, whose elements are in one-to-one correspondence with $\tilde{\Omega}(\nu)$, where $\nu$ does not exceed the topological invariant $\nu_0$. The value $\omega_i$ can be viewed as the number of "small" rotations made by the orbit near the saddle after the $i$th "global" turn.

(2) As $\beta$ approaches zero taking positive or negative values, an *infinite* number of bifurcations results. Some of these bifurcations are related to a "basic" limit cycle, which makes one global turn along the homoclinic

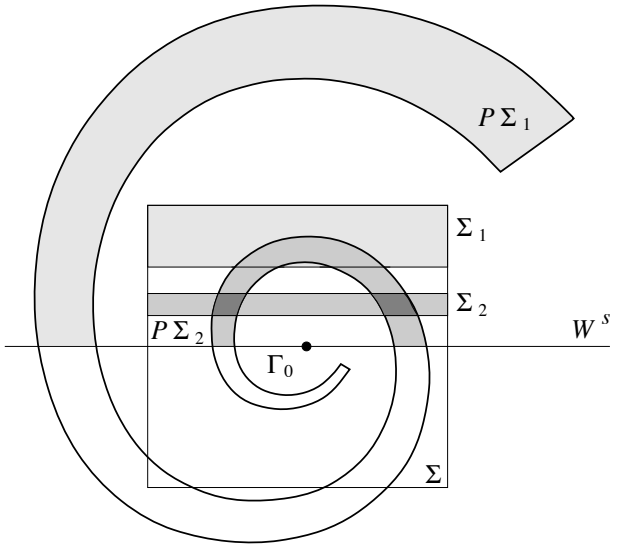


(a)

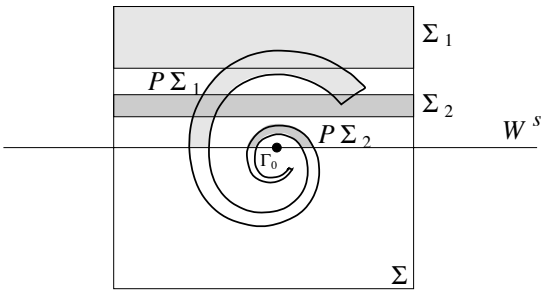


(b)

FIGURE 6.33. Poincaré map structure in the saddle-focus cases: (a) $\sigma_0 > 0$; (b) $\sigma_0 < 0$.

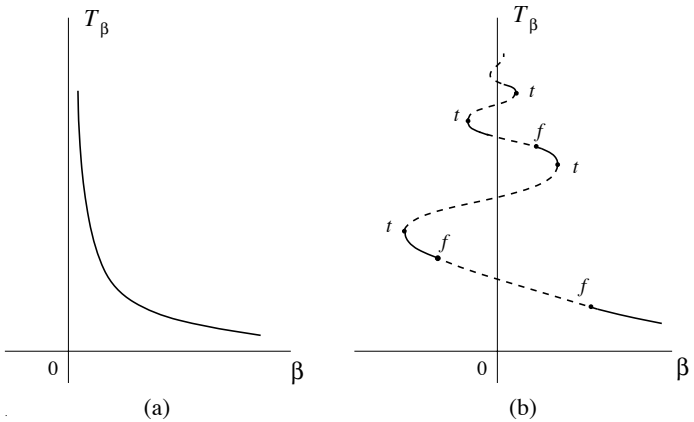


FIGURE 6.34. Period of the cycle near a saddle-focus homoclinic bifurcation: (a) $\sigma_0 < 0$; (b) $\sigma_0 > 0$.

orbit. It can be shown that this cycle undergoes an infinite number of *tangent* bifurcations as $|\beta|$ tends to zero. To understand the phenomenon, it is useful to compare the dependence on $\beta$ of the period $T_\beta$ of the cycle in the saddle-focus cases with $\sigma_0 < 0$ and $\sigma_0 > 0$. The relevant graphs are presented in Figure 6.34. In the $\sigma_0 < 0$ case, the dependence is monotone, while if $\sigma_0 > 0$ it becomes "wiggly." The presence of wiggles means that the basic cycle disappears and appears via tangent (fold) bifurcations infinitely many times. Notice that for any sufficiently small $|\beta|$ there is only a finite number of these "basic" cycles (they differ in the number of "small" rotations near the saddle-focus; the higher the period, the more rotations the cycle has). Moreover, the cycle also exhibits an infinite number of *period-doubling* bifurcations. The tangent and flip bifurcations are marked by $t$ and $f$, respectively, in the figure. The flip bifurcations generate double-period cycles. Each of them makes two global turns before closure. These cycles themselves bifurcate while approaching the homoclinic orbit, making the picture more involved. The basic cycle, as well as the secondary cycles generated by period doublings, are *stable* or *repelling*, depending on the sign of the divergence of (6.17) at the saddle-focus:

$$\sigma_1 = (\text{div } f)(x_0, 0) = \lambda_1 + \lambda_2 + \lambda_3 = \lambda_1 + 2 \text{ Re } \lambda_{2,3}.$$

If $\sigma_1 < 0$ the basic cycle near the bifurcation can be stable (actually, there are only short intervals of $\beta$ within which it is stable). If $\sigma_1 > 0$ there are intervals where the basic cycle is totally unstable (repelling). Thus, the saddle cycles mentioned in the theorem and coded at $\beta = 0$ by periodic sequences of $\Omega(\nu)$ are not the *only* cycles in $U_0$.

(3) Other bifurcations near the homoclinic orbit are due to *secondary homoclinic orbits*. Under the conditions of Theorem 6.5, there is an infinite sequence of $\beta_i > 0$, $\beta_i \to 0$, for which the system has double homoclinic

orbits with different (increasing) number of rotations near the saddle-focus (see Figure 6.35). Other subsidiary homoclinic orbits are also present, like the triple making three global turns before final return.

(4) Recall that in this section we assumed $n_- = \dim W^s = 2$ and $n_+ = \dim W^u = 1$. To apply the results in the opposite case (i.e., $n_- = 1, n_+ = 2$), we have to reverse the direction of time. This boils down to these substitutions: $\lambda_j \mapsto -\lambda_j,\ \sigma_i \mapsto -\sigma_i$, and "stable" $\mapsto$ "repelling." $\diamondsuit$

**Example 6.3 (Complex impulses in the FitzHugh-Nagumo model)** The following system of partial differential equations is the FitzHugh-Nagumo caricature of the Hodgkin-Huxley equations modeling the nerve impulse propagation along an axon (FitzHugh [1961], Nagumo, Arimoto & Yoshizawa [1962]):

$$\begin{aligned} \frac{\partial u}{\partial t} &= \frac{\partial^2 u}{\partial x^2} - f_a(u) - v, \\ \frac{\partial v}{\partial t} &= bu, \end{aligned}$$

where $u = u(x,t)$ represents the membrane potential; $v = v(x,t)$ is a phenomenological "recovery" variable; $f_a(u) = u(u-a)(u-1),\ 1 > a > 0,\ b > 0,\ -\infty < x < +\infty,\ t > 0$.

*Traveling waves* are solutions to these equations of the form

$$u(x,t) = U(\xi),\ v(x,t) = V(\xi),\ \xi = x + ct,$$

where $c$ is an a priori unknown wave propagation speed. The functions $U(\xi)$ and $V(\xi)$ define profiles of the waves. They satisfy the following system of ordinary differential equations:

$$\left\{ \begin{array}{rcl} \dot{U} &=& W, \\ \dot{W} &=& cW + f_a(U) + V, \\ \dot{V} &=& \frac{b}{c}U, \end{array} \right. \tag{6.18}$$

where the dot means differentiation with respect to "time" $\xi$. System (6.18) is called a *wave system*. It depends on three positive parameters $(a, b, c)$.

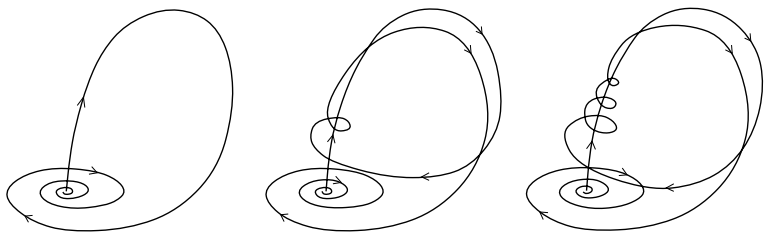


FIGURE 6.35. Basic (a) and double (b, c) homoclinic orbits.

Any bounded orbit of (6.18) corresponds to a traveling wave solution of the FitzHugh-Nagumo system at parameter values $(a, b)$ propagating with velocity $c$.

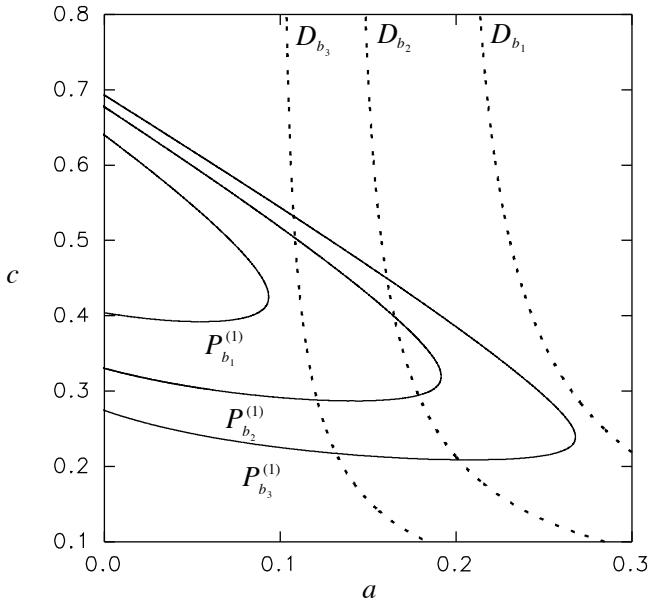


FIGURE 6.36. Bifurcation curves of the wave system (6.16): $b_1 = 0.01$; $b_2 = 0.005$; $b_3 = 0.0025$.

For all $c > 0$ the wave system has a unique equilibrium $0 = (0, 0, 0)$ with one positive eigenvalue $\lambda_1$ and two eigenvalues $\lambda_{2,3}$ with negative real parts (see Exercise 2 in Chapter 2). The equilibrium can be either a saddle or a saddle-focus with a one-dimensional unstable and a two-dimensional stable invariant manifold, $W^{u,s}(0)$. The transition between saddle and saddle-focus cases is caused by the presence of a double negative eigenvalue; for fixed $b > 0$ this happens on the curve

$$D_b = \{(a, c) : c^4(4b - a^2) + 2ac^2(9b - 2a^2) + 27b^2 = 0\}.$$

Several boundaries $D_b$ in the $(a, c)$-plane for different values of $b$ are depicted in Figure 6.36 as dotted lines. The saddle-focus region is located below each boundary and disappears as $b \to 0$.

A branch $W_1^u(0)$ of the unstable manifold leaving the origin into the positive octant can return back to the equilibrium, forming a homoclinic orbit $\Gamma_0$ at some parameter values [Hastings 1976]. These parameter values can be found only numerically with the help of the methods described in Chapter 10. Figure 6.36 presents several homoclinic bifurcation curves $P_b^{(1)}$ in the $(a, c)$-plane computed by Kuznetsov & Panfilov [1981] for different

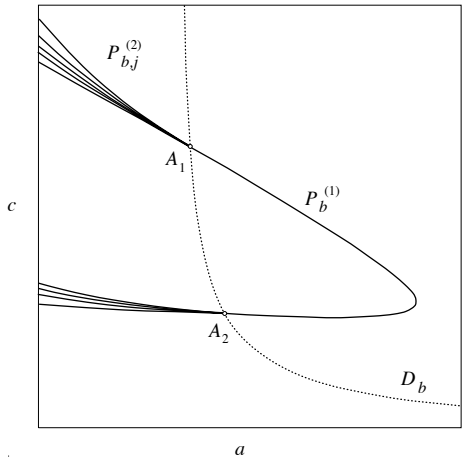


FIGURE 6.37. Parametric curves $D_b$ and $P_b^{(1)}$ for $b = 0.0025$.

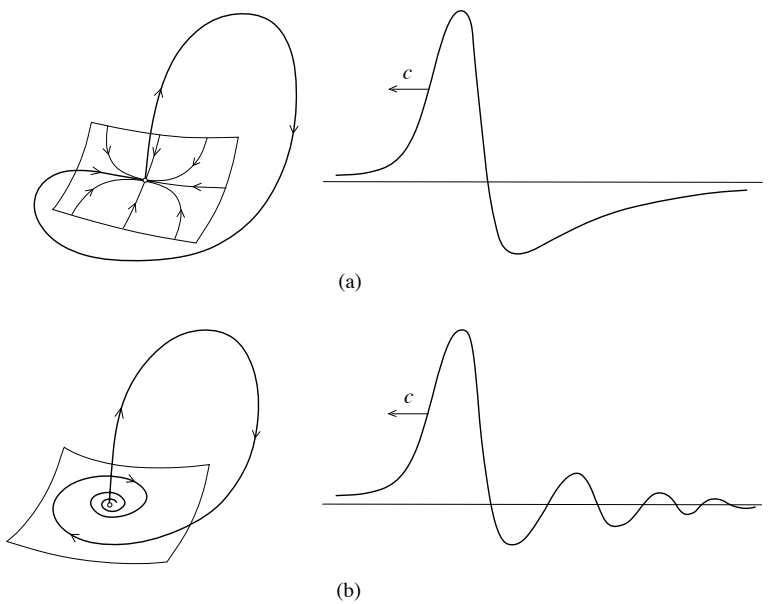


FIGURE 6.38. Impulses with (a) monotone and (b) oscillating "tails".

but fixed values of $b$. Looking at Figure 6.36, we can conclude that for all $b > 0$ the bifurcation curve $P_b^{(1)}$ passes through the saddle-focus region delimited by $D_b$ (see Figure 6.37, where the curves $D_b$ and $P_b^{(1)}$ corresponding to $b = 0.0025$ are superimposed). Actually, for $b > 0.1$, the homoclinic bifurcation curve belongs entirely to the saddle-focus region. Any homoclinic orbit defines a traveling *impulse*. The shape of the impulse depends very much on the type of the corresponding equilibrium: It has a monotone "tail" in the saddle case and an oscillating "tail" in the saddle-focus case (see Figure 6.38).

The saddle quantity $\sigma_0$ is always positive for $c > 0$ (see Exercise 11). Therefore, the phase portraits of (6.14) near the homoclinic curve $P_b^{(1)}$ are described by Theorems 6.4 and 6.5. In particular, near the homoclinic bifurcation curve $P_b^{(1)}$ in the saddle-focus region, system (6.18) has an infinite number of saddle cycles. These cycles correspond to *periodic wave trains* in the FitzHugh-Nagumo model [Feroe 1981]. Secondary homoclinic orbits existing in (6.18) near the primary homoclinic bifurcation correspond to *double traveling impulses* (see Figure 6.39) [Evans, Fenichel & Feroe 1982]. It can be shown using results by Belyakov [1980] (see Kuznetsov

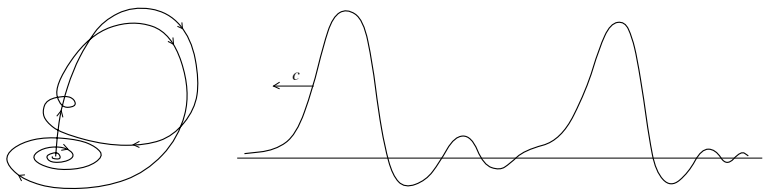


FIGURE 6.39. A double impulse.

& Panfilov [1981]) that secondary homoclinic bifurcation curves $P_{b,j}^{(2)}$ in (6.18) originate at points $A_{1,2}$ where $P_b^{(1)}$ intersects $D_b$ (see Figure 6.37 for a sketch). $\diamond$

## 6.4 Homoclinic bifurcations in $n$-dimensional systems

It has been proved (see references in Appendix 2) that there exists a parameter-dependent invariant *center manifold* near homoclinic bifurcations. This allows one to reduce the study of generic bifurcations of orbits homoclinic to hyperbolic equilibria in $n$-dimensional systems with $n > 3$ to that in two-, three-, or four-dimensional systems. In this section, we discuss which homoclinic orbits are generic in $n$-dimensional case and formulate the *Homoclinic Center Manifold Theorem* for such orbits. Then we derive from this theorem some results concerning generic homoclinic bifur-

cations in $n$-dimensional systems, first obtained by L.P. Shil'nikov without a center-manifold reduction.

### *6.4.1 Regular homoclinic orbits: Melnikov integral*

Consider a system

$$\dot{x} = f(x,\alpha), \quad x = (x_1, x_2, \dots, x_n)^T \in \mathbb{R}^n, \ \alpha \in \mathbb{R}^1, \tag{6.19}$$

where $f$ is $C^\infty$ smooth and $n \geq 3$. Suppose, that (6.19) has a hyperbolic equilibrium $x_0$ at $\alpha = 0$, and the Jacobian matrix $A_0 = f_x(x_0, 0)$ has $n_+$ eigenvalues with positive real parts

$$0 < \ \mathrm{Re}\ \lambda_1 \ \leq \ \mathrm{Re}\ \lambda_2 \ \leq \cdots \leq \ \mathrm{Re}\ \lambda_{n_+}$$

and $n_-$ eigenvalues with negative real parts

$$\mathrm{Re}\ \mu_{n_-} \ \leq \ \mathrm{Re}\ \mu_{n_- - 1} \ \leq \cdots \leq \ \mathrm{Re}\ \mu_1 < 0.$$

For all sufficiently small $|\alpha|$, the equilibrium persists and has unstable and stable local invariant manifolds $W^u$ and $W^s$ that can be globally extended, $\dim W^{u,s} = n_\pm, \ n_+ + n_- = n$. Assume that (6.19) has at $\alpha = 0$ an orbit $\Gamma_0$ homoclinic to $x_0$ and denote by $x^0(t)$ a solution of (6.19) corresponding to $\Gamma_0$.

As we have seen in Section 6.1, the intersection of $W^s(x_0)$ and $W^u(x_0)$ along $\Gamma_0$ cannot be transversal, since the vector $\dot{x}^0(t_0) = f(x^0(t_0), 0)$ is tangent to both manifolds at any point $x^0(t_0) \in \Gamma_0$. However, in the generic case, $\dot{x}^0(t_0)$ is the only such vector:

$$T_{x^0(t_0)} W^u(x_0) \cap T_{x^0(t_0)} W^s(x_0) = \mathrm{span}\{\dot{x}^0(t_0)\}.$$

Thus, generically,

$$\mathrm{codim}(T_{x^0(t_0)} W^s(x_0) + T_{x^0(t_0)} W^s(x_0)) = 1.$$

A generic perturbation splits the manifolds $W^s(x_0)$ and $W^u(x_0)$ by an $O(\alpha)$-distance in the remaining direction for $\alpha \neq 0$. Such homoclinic orbits are called *regular*.

As in Section 6.2, introduce the *extended system*:

$$\left\{ \begin{array}{rcl} \dot{x} & = & f(x,\alpha), \\ \dot{\alpha} & = & 0, \end{array} \right. \tag{6.20}$$

with the phase variables $(x,\alpha)^T \in \mathbb{R}^{n+1}$. Let $x_0(\alpha)$ denote a one-parameter family of the saddles in (6.19) for small $|\alpha|$, $x_0(0) = x_0$. This family defines an invariant set of (6.20) – a curve of equilibria. This curve has the unstable and stable manifolds, $\mathcal{W}^u$ and $\mathcal{W}^s$, whose slices $\alpha = \mathrm{const}$ coincide with

the corresponding unstable and stable manifolds $W^u$ and $W^s$ of the saddle $x_0(\alpha)$. It is clear that the regularity of the homoclinic orbit translates exactly into the *transversality* of the intersection of $\mathcal{W}^u$ and $\mathcal{W}^s$ along $\Gamma_0$ at $\alpha = 0$ in the $(n+1)$-dimensional phase space of (6.20):

$$T_{(x^0(t_0),0)}\mathcal{W}^u + T_{(x^0(t_0),0)}\mathcal{W}^s = \mathbb{R}^{n+1}.$$

Figure 6.22 in Section 6.2 illustrates the case $n = 2$.

The transversality of the intersection of $\mathcal{W}^u$ and $\mathcal{W}^s$ can be expressed analytically. Namely, consider the *linearization* of (6.20) around $x^0(t)$ at $\alpha = 0$:

$$\left\{ \begin{array}{rcl} \dot{u} & = & f_x(x^0(t),0)u + f_\alpha(x^0(t),0)\mu, \\ \dot{\mu} & = & 0. \end{array} \right. \tag{6.21}$$

If $(u_0, \mu_0)^T$ is a vector tangent to either $\mathcal{W}^u$ or $\mathcal{W}^s$, then the solution vector $(u(t), \mu(t))^T$ of this system with the initial data $(u_0, \mu_0)^T$ is always tangent to the corresponding invariant manifold. The vector function

$$\left( \begin{array}{c} \zeta(t) \\ \mu(t) \end{array} \right) = \left( \begin{array}{c} \dot{x}^0(t) \\ 0 \end{array} \right)$$

is a bounded solution to (6.21) that is tangent to both invariant manifolds $\mathcal{W}^u$ and $\mathcal{W}^s$ along the curve of their intersection.[8] We can multiply this solution by a scalar to get another bounded solution to (6.21). The transversality of the intersection of $\mathcal{W}^u$ and $\mathcal{W}^s$ along $\Gamma_0$ at $\alpha = 0$ means that $(\dot{x}^0(t), 0)^T$ is the unique to within a scalar multiple bounded solution to the extended system (6.21). Taking into account that the equation for $\mu$ in (6.21) is trivial, we can conclude that $\dot{x}^0(t)$ is the unique to within a scalar multiple solution to the *variational equation* around $\Gamma_0$:

$$\dot{u} = A(t)u, \quad u \in \mathbb{R}^n, \tag{6.22}$$

where $A(t) = f_x(x^0(t), 0)$. This implies that the *adjoint variational equation* around $\Gamma_0$:

$$\dot{v} = -A^T(t)v, \quad v \in \mathbb{R}^n, \tag{6.23}$$

has the unique to within a scalar multiple bounded solution $v(t) = \eta(t)$. Indeed, if $X(t)$ is the fundamental matrix solution to (6.22), i.e., $\dot{X}(t) = A(t)X(t)$, $X(0) = I_n$, then $Y(t) = [X^T(t)]^{-1}$ is the fundamental matrix solution to (6.23), so equations (6.22) and (6.23) have the same number of linearly independent bounded solutions. Actually, the vectors $\zeta(t)$ and $\eta(t)$ are orthogonal for each $t \in \mathbb{R}^1$. Using (6.22) and (6.23), we get

$$\frac{d}{dt}\langle \eta, \zeta \rangle = \langle \dot{\eta}, \zeta \rangle + \langle \eta, \dot{\zeta} \rangle = -\langle A^T\eta, \zeta \rangle + \langle \eta, A\zeta \rangle = -\langle \eta, A\zeta \rangle + \langle \eta, A\zeta \rangle = 0,$$

[8] Actually, this solution tends to zero exponentially fast as $t \to \pm\infty$ since $\dot{x}^0(t) = f(x^0(t), 0)$.

i.e., $\langle \eta(t), \zeta(t) \rangle = C$. The constant $C$ is zero, since both $\eta(t)$ and $\zeta(t)$ tend to zero exponentially fast as $t \to \pm\infty$:

$$\langle \eta(t), \zeta(t) \rangle = 0, \quad t \in \mathbb{R}^1.$$

Meanwhile, similar arguments show that $\eta(t)$ is orthogonal to any vector tangent to either $W^s(x_0)$ or $W^u(x_0)$. Moreover, the transversality is equivalent to the condition

$$M_\alpha(0) = \int_{-\infty}^{+\infty} \langle \eta(t), f_\alpha(x^0(t), 0) \rangle \, dt \neq 0. \tag{6.24}$$

If the intersection of $\mathcal{W}^u$ and $\mathcal{W}^s$ is nontransversal, there exists another bounded solution $(\zeta_0(t), \mu_0)^T$ to (6.21) with $\mu_0 \neq 0$. Taking the scalar product of (6.21) with $\eta$ and integrating over time, we get

$$\begin{aligned} \mu_0 \int_{-\infty}^{+\infty} \langle \eta(t), f_\alpha(x^0(t), 0) \rangle \, dt &= \int_{-\infty}^{+\infty} \langle \eta(t), \dot{\zeta}_0(t) - A(t)\zeta_0(t) \rangle \, dt \\ = \langle \eta(t), \zeta_0(t) \rangle|_{-\infty}^{+\infty} - \int_{-\infty}^{+\infty} \langle \dot{\eta}(t) + A^T(t)\eta(t), \zeta_0(t) \rangle \, dt &= 0. \end{aligned}$$

The integral in (6.24) is called the *Melnikov integral*. This condition allows us to verify the regularity of the manifold splitting in $n$-dimensional systems with $n \geq 2$. Moreover, one can introduce a scalar split function $M(\alpha)$ that measures the displacement of the invariant manifolds $W^s(x_0)$ and $W^u(x_0)$ near the point $x^0(0) \in \Gamma_0$ in the direction defined by the vector $\eta(0)$ and has the property

$$M(\alpha) = M_\alpha(0)\alpha + O(\alpha^2),$$

where $M_\alpha(0)$ is given by (6.24).

In the two-dimensional case the Melnikov integral $M_\alpha(0)$ can be computed more explicitly. Write (6.19) in coordinates:

$$\begin{cases} \dot{x}_1 = f_1(x, \alpha), \\ \dot{x}_2 = f_2(x, \alpha). \end{cases}$$

The solution $\zeta(t)$ to the variational equation (6.22) has the form

$$\zeta(t) = \dot{x}^0(t) = \begin{pmatrix} f_1(x^0(t), 0) \\ f_2(x^0(t), 0) \end{pmatrix}.$$

Since $\eta(t) \perp \zeta(t)$, we have

$$\eta(t) = \varphi(t) \begin{pmatrix} -f_2(x^0(t), 0) \\ f_1(x^0(t), 0) \end{pmatrix}$$

for some scalar function $\varphi(t)$. It is easy to verify that this function satisfies the equation

$$\dot{\varphi}(t) = -(\text{div } f)(x^0(t), 0)\varphi(t),$$

where

$$\text{div } f = \left(\frac{\partial f_1}{\partial x_1} + \frac{\partial f_2}{\partial x_2}\right)$$

is the *divergence* of the vector field $f$. Assuming $\varphi(0) = 1$, we obtain

$$\varphi(t) = e^{-\int_0^t (\text{div } f)(x^0(\tau),0)\, d\tau}$$

and

$$M_\alpha(0) = \int_{-\infty}^{+\infty} \exp\left[-\int_0^t \left(\frac{\partial f_1}{\partial x_1} + \frac{\partial f_2}{\partial x_2}\right) d\tau\right] \left(f_1 \frac{\partial f_2}{\partial \alpha} - f_2 \frac{\partial f_1}{\partial \alpha}\right) dt, \tag{6.25}$$

where all expressions with $f = (f_1, f_2)^T$ are evaluated along the homoclinic solution $x^0(\cdot)$ at $\alpha = 0$.

**Remark:**

Suppose that (6.4) is a Hamiltonian system at $\alpha = 0$, and $\alpha$ is a small parameter in front of the perturbation, i.e.,

$$\dot{x} = J(\nabla H)(x) + \alpha g(x), \quad x \in \mathbb{R}^2,\ \alpha \in \mathbb{R}^1,$$

where

$$J = \begin{pmatrix} 0 & 1 \\ -1 & 0 \end{pmatrix}, \quad \nabla H = \left(\frac{\partial H}{\partial x_1}, \frac{\partial H}{\partial x_2}\right)^T,$$

and $H = H(x)$ is the Hamiltonian function. Then the Melnikov integral (6.25) can be simplifyed further. In such a case, div $f \equiv 0$ and the homoclinic orbit $\Gamma_0$ belongs to a level curve $\{x : H(x) = H(x_0)\}$. Assume that its interior is a domain $\Omega = \{H(x) \le H(x_0)\}$. Then, applying Green's theorem reduces the Melnikov integral along $\Gamma_0$ to the following domain integral:

$$M_\alpha(0) = \int_\Omega (\text{div } g)(x^0(t))\, d\omega. \ \diamondsuit$$

### *6.4.2 Homoclinic center manifolds*

To formulate the Homoclinic Center Manifold Theorem, it is useful to distinguish the eigenvalues that are closest to the imaginary axis (see Figure 6.40).

**Definition 6.9** *The eigenvalues with positive* (*negative*) *real part that are closest to the imaginary axis are called the unstable* (*stable*) leading eigenvalues, *while the corresponding eigenspaces are called the unstable* (*stable*) leading eigenspaces.

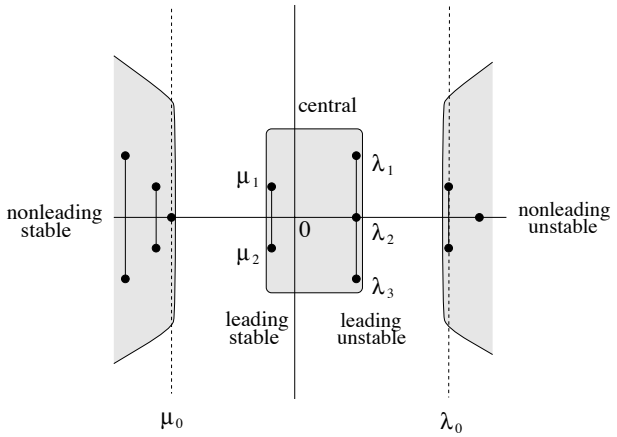


FIGURE 6.40. Splitting of the eigenvalues.

**Definition 6.10** *The stable and unstable leading eigenvalues together are called* central eigenvalues*, while the corresponding eigenspace is called the* central eigenspace.

Almost all orbits on $W^u(W^s)$ tend to the equilibrium as $t \to -\infty$ ($t \to +\infty$) along the corresponding leading eigenspace that we denote by $T^u(T^s)$. Exceptional orbits form a *nonleading* manifold $W^{uu}(W^{ss})$ tangent to the eigenspace $T^{uu}(T^{ss})$ corresponding to the nonleading eigenvalues. The central eigenspace $T^c$ is the direct sum of the stable and unstable leading eigenspaces: $T^c = T^u \oplus T^s$. Denote by $\lambda_0$ the minimal Re $\lambda_j$ corresponding to the *nonleading* unstable eigenvalues and by $\mu_0$ the maximal Re $\mu_j$ corresponding to the *nonleading* stable eigenvalues (see Figure 6.40). By the construction,

$$\mu_0 < \text{Re } \mu_1 < 0 < \text{Re } \lambda_1 < \lambda_0,$$

where $\lambda_1$ is a leading unstable eigenvalue and $\mu_1$ is a leading stable eigenvalue. Provided both nonleading eigenspaces are nonempty, introduce two real numbers:

$$g^s = \frac{\mu_0}{\text{Re } \mu_1}, \quad g^u = \frac{\lambda_0}{\text{Re } \lambda_1}.$$

These numbers characterize the *relative gaps* between the corresponding nonleading and leading eigenvalues and satisfy $g^{s,u} > 1$. If one of the nonleading eigenspaces is empty, set formally $g^s = -\infty$ or $g^u = +\infty$.

Now notice that the variational equation (6.22) is a nonautonomous linear system with matrix $A(t)$ that approaches asymptotically a constant matrix, namely

$$\lim_{t \to \pm\infty} A(t) = A_0.$$

Therefore, for $t \to \pm\infty$, solutions of (6.21) behave like solutions of the autonomous linear system

$$\dot{v} = A_0 v$$

and we can introduce four linear subspaces of $\mathbb{R}^n$:

$$\begin{aligned} E^{uu}(t_0) &= \left\{ v_0 : \lim_{t\to-\infty} \frac{v(t)}{\|v(t)\|} \in T^{uu} \right\}, \\ E^{ss}(t_0) &= \left\{ v_0 : \lim_{t\to+\infty} \frac{v(t)}{\|v(t)\|} \in T^{ss} \right\}, \end{aligned}$$

$$\begin{aligned} E^{cu}(t_0) &= \left\{ v_0 : \lim_{t\to-\infty} \frac{v(t)}{\|v(t)\|} \in T^{c} \oplus T^{uu} \right\}, \\ E^{cs}(t_0) &= \left\{ v_0 : \lim_{t\to+\infty} \frac{v(t)}{\|v(t)\|} \in T^{c} \oplus T^{ss} \right\}, \end{aligned}$$

where $v(t) = \Phi(v_0, t_0, t)$ is the solution to (6.21) with the initial data $v = v_0$ at $t = t_0$, and $\oplus$ stands for the direct sum of the linear subspaces. Finally, define

$$E^c(t_0) = E^{cu}(t_0) \cap E^{cs}(t_0).$$

Now we can formulate without proof the following theorem.

**Theorem 6.7 (Homoclinic Center Manifold)** *Suppose that* (6.19) *has at* $\alpha = 0$ *a hyperbolic equilibrium* $x_0 = 0$ *with a homoclinic orbit*

$$\Gamma_0 = \{x \in \mathbb{R}^n : \ x = x^0(t), \ t \in \mathbb{R}^1\}.$$

*Assume the following conditions hold*:

(H.1) $\dot{x}^0(0) \in E^c(0)$;
(H.2) $E^{uu}(0) \oplus E^c(0) \oplus E^{ss}(0) = \mathbb{R}^n$.

*Then, for all sufficiently small* $|\alpha|$, (6.19) *has an invariant manifold* $\mathcal{M}_\alpha$ *defined in a small neighborhood* $U_0$ *of* $\Gamma_0 \cup x_0$ *and having the following properties*:

(i) $x^0(t_0) \in \mathcal{M}_0$ *and the tangent space* $T_{x^0(t_0)}\mathcal{M}_0 = E^c(t_0)$, *for all* $t_0 \in \mathbb{R}^1$;

(ii) *any solution to* (6.19) *that stays inside* $U_0$ *for all* $t \in \mathbb{R}^1$ *belongs to* $\mathcal{M}_\alpha$;

(iii) *each* $\mathcal{M}_\alpha$ *is* $C^k$ *smooth, where* $k \geq 1$ *is the maximal integer number satisfying both*

$$g^s > k \quad \textit{and} \quad g^u > k. \quad \square$$

**Definition 6.11** *The manifold* $\mathcal{M}_\alpha$ *is called the* homoclinic center manifold.

**Remarks:**

(1) The conditions (H.1) and (H.2) guarantee that similar conditions hold for all $t_0 \neq 0$. The first condition implies that the homoclinic orbit $\Gamma_0$ approaches the equilibrium $x_0$ along the leading eigenspaces for both $t \to +\infty$ and $t \to -\infty$. The second condition means that the invariant manifolds $W^s(x_0)$ and $W^u(x_0)$ intersect at $\alpha = 0$ along the homoclinic orbit $\Gamma_0$ in the "least possible" nontransversal manner.

(2) The manifold $\mathcal{M}_0$ is exponentially attracting along the $E^{ss}$-directions and exponentially repelling along the $E^{uu}$-directions. The same property holds for $\mathcal{M}_\alpha$ for small $|\alpha| \neq 0$ with $E^{ss,uu}$ replaced by close subspaces.

(3) The homoclinic center manifold has only *finite smoothness* $C^k$ that increases with the relative gaps $g^{s,u}$. The restriction of (6.19) to the invariant manifold $\mathcal{M}_\alpha$ is a $C^k$-system of ODEs, provided proper coordinates on $\mathcal{M}_\alpha$ are choosen. This restricted system has an orbit homoclinic to $x_0$ at $\alpha = 0$.

(4) Actually, under the assumptions of Theorem 6.7, the homoclinic center manifold belongs to the class $C^{k,\beta}$ with some $0 < \beta < 0$, i.e., can locally be represented as the graph of a function whose derivatives of order $k$ are Hölder-continuous with index $\beta$. $\diamondsuit$

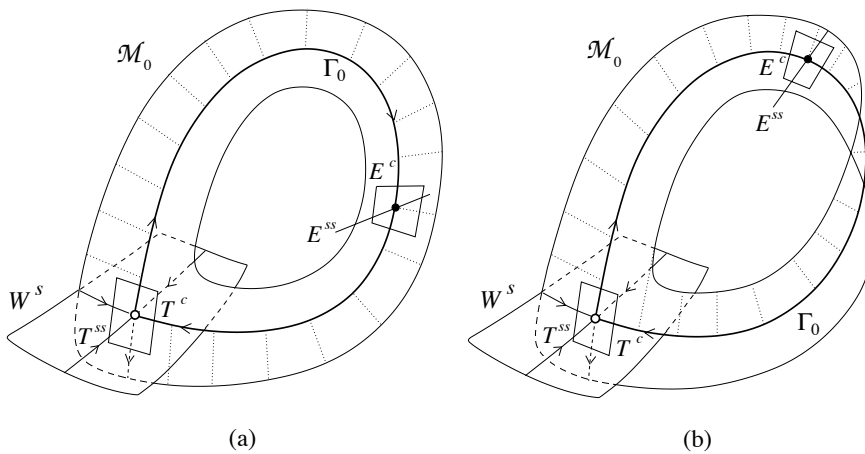


FIGURE 6.41. Homoclinic center manifold in $\mathbb{R}^3$.

The theorem is illustrated for $\mathbb{R}^3$ in Figure 6.41. Only the critical homoclinic center manifold $\mathcal{M}_0$ at $\alpha = 0$ is presented. It is assumed that all eigenvalues of $x_0$ are real and simple: $\mu_2 < \mu_1 < 0 < \lambda_1$. The central eigenspace $T^c$ of the saddle $x_0$ is two-dimensional and is spanned by the (leading) unstable eigenvector $v_1$ ($A_0 v_1 = \lambda_1 v_1$) and the leading stable eigenvector $w_1$ ($A_0 w_1 = \mu_1 w_1$). The manifold $\mathcal{M}_0$ is two-dimensional, contains $\Gamma_0$, and is tangent to $T^c$ at $x_0$. It is exponentially attracting in the $E^{ss}$-direction. The manifold can be either *orientable* (Figure 6.41(a)) or

*nonorientable* (Figure 6.41(b)). In this case, condition (H.2) is equivalent to the strong inclination property (see Section 6.3), so the orientability of $\mathcal{M}_0$ depends on whether the closure of $W^u$ near $\Gamma_0$ is orientable or nonorientable (cf. Figure 6.26).

### *6.4.3 Generic homoclinic bifurcations in* $\mathbb{R}^n$

Generically, the leading eigenspaces $T^{s,u}$ are either one- or two-dimensional. In the first case, an eigenspace corresponds to a simple real eigenvalue, while in the second case, it corresponds to a simple pair of complex-conjugate eigenvalues. Reversing the time direction if necessary, we have only three typical configurations of the leading eigenvalues:

(a) (*saddle*) The leading eigenvalues are real and simple: $\mu_1 < 0 < \lambda_1$ (Figure 6.42(a));
(b) (*saddle-focus*) The stable leading eigenvalues are complex and simple: $\mu_1 = \bar{\mu}_2$, while the unstable leading eigenvalue $\lambda_1$ is real and simple (Figure 6.42(b));
(c) (*focus-focus*) The leading eigenvalues are complex and simple: $\lambda_1 = \bar{\lambda}_2,\ \mu_1 = \bar{\mu}_2$ (Figure 6.42(c)).

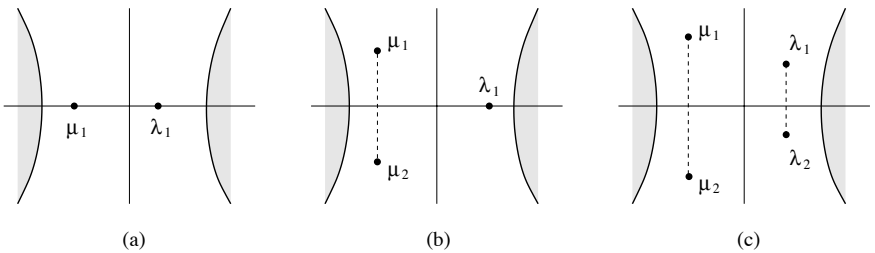


FIGURE 6.42. Leading eigenvalues in generic Shil'nikov cases.

**Definition 6.12** *The saddle quantity $\sigma$ of a hyperbolic equilibrium is the sum of the real parts of its leading eigenvalues.*

Therefore,

$$\sigma = \operatorname{Re} \lambda_1 + \operatorname{Re} \mu_1,$$

where $\lambda_1$ is a leading unstable eigenvalue and $\mu_1$ is a leading stable eigenvalue. Assume that the following nondegeneracy condition holds at $\alpha = 0$:

(H.0) $\sigma_0 \neq 0$ *and the leading eigenspaces $T^{s,u}$ are either one- or two-dimensional.*

The following theorems are direct consequences of Theorem 6.7 and the results obtained in Sections 6.2–6.4.

**Theorem 6.8 (Saddle)** *For any generic one-parameter system having a saddle equilibrium point $x_0$ with a homoclinic orbit $\Gamma_0$ at $\alpha = 0$ there exists a neighborhood $U_0$ of $\Gamma_0 \cup x_0$ in which a unique limit cycle $L_\alpha$ bifurcates from $\Gamma_0$ as $\alpha$ passes through zero. Moreover,* $\dim W^s(L_\alpha) = n_- + 1$ *if* $\sigma_0 < 0$, *and* $\dim W^s(L_\alpha) = n_-$ *if* $\sigma_0 > 0$. □

In the saddle case, the homoclinic center manifold $\mathcal{M}_\alpha$ is two-dimensional and is a simple (orientable) or a twisted (nonorientable or Möbius) band. At $\alpha = 0$ the restricted system has a homoclinic orbit. The proof of Theorem 6.2 (see Section 6.2) can be carried out with only a slight modification. Namely, the coefficient $a(\beta)$ of the global map $Q$ can now be either positive (orientable case) or negative (Möbius case). In this case conditions (H.1) and (H.2) imply that the $W^{u,s}$ intersects itself near the saddle along the corresponding nonleading manifold $W^{ss,uu}$. In the three-dimensional case this condition means that the homoclinic orbit $\Gamma_0$ is either simple or twisted (as defined in Section 6.3). Thus, we have an alternative way to prove Theorems 6.2 and 6.4.

**Theorem 6.9 (Saddle-focus)** *For any generic one-parameter system having a saddle-focus equilibrium point $x_0$ with a homoclinic orbit $\Gamma_0$ at $\alpha = 0$ there exists a neighborhood $U_0$ of $\Gamma_0 \cup x_0$ such that one of the following alternatives hold:*

(a) *if $\sigma_0 < 0$, a unique limit cycle $L_\alpha$ bifurcates from $\Gamma_0$ in $U_0$ as $\alpha$ passes through zero,* $\dim W^s(L_\alpha) = n_- + 1$;

(b) *if $\sigma_0 > 0$, the system has an infinite number of saddle limit cycles in $U_0$ for all sufficiently small $|\alpha|$.* □

In this case, the homoclinic center manifold $\mathcal{M}_\alpha$ is three-dimensional. At $\alpha = 0$ the restricted system has a homoclinic orbit to the saddle-focus, so we can repeat the proof of Theorem 6.5 (in case (a)) and that of Theorem 6.5 (in case (b)) on this manifold.

**Theorem 6.10 (Focus-focus)** *For any generic one-parameter system having a focus-focus equilibrium point $x_0$ with a homoclinic orbit $\Gamma_0$ at $\alpha = 0$ there exists a neighborhood $U_0$ of $\Gamma_0 \cup x_0$ in which the system has an infinite number of saddle limit cycles in $U_0$ for all sufficiently small $|\alpha|$.* □

Here, the homoclinic center manifold $\mathcal{M}_\alpha$ is four-dimensional and carries a homoclinic orbit to the focus-focus at $\alpha = 0$. Thus, the proof of Theorem 6.11 from Appendix 1 is valid.

The genericity conditions mentioned in the theorems are the nondegeneracy conditions (H.0), (H.1), and (H.2) listed above, as well as the transversality condition:

(H.3) *the homoclinic orbit $\Gamma_0$ is regular, i.e., the intersection of the tangent spaces $T_{x^0(t)}W^s$ and $T_{x^0(t)}W^u$ at each point $x^0(t) \in \Gamma_0$ is one-dimensional and $W^s$ and $W^u$ split by an $O(\alpha)$ distance as $\alpha$ moves away from zero.*

Recall that $(H.3)$ can be reformulated using the Melnikov integral as

$$\int_{-\infty}^{+\infty} \langle \eta(t), f_\alpha(x^0(t), 0) \rangle \, dt \neq 0,$$

where $\eta(t)$ is the unique to within a scalar multiple bounded solution to the *adjoint variational equation* around $\Gamma_0$:

$$\dot{u} = -A^T(t)u, \quad u \in \mathbb{R}^n.$$

## 6.5 Exercises

**(1)** Construct a one-parameter family of two-dimensional Hamiltonian systems

$$\begin{cases} \dot{x} = H_y, \\ \dot{y} = -H_x, \end{cases}$$

where $H = H(x, y, \alpha)$ is a (polynomial) Hamilton function, having a homoclinic orbit. (*Hint*: Orbits of the system belong to level curves of the Hamiltonian: $H(x, y, \alpha) = \text{const.}$)

**(2) (Homoclinc orbit in a non-Hamiltonian system)** Show that the system

$$\begin{cases} \dot{x} = y, \\ \dot{y} = x^3 + x + xy, \end{cases}$$

has a saddle at the origin with a "big" homoclinic orbit. (*Hint*: Use the symmetry of the system under a reflection and time reversal: $x \mapsto -x$, $t \mapsto -t$.) Is this orbit nondegenerate?

**(3)** Prove Lemma 6.1 in the planar case using rotation of the vector field. (*Hint*: See Andronov et al. [1973].)

**(4) (Heteroclinic bifurcation)** Prove that the system

$$\begin{cases} \dot{x} = \alpha + 2xy, \\ \dot{y} = 1 + x^2 - y^2, \end{cases}$$

undergoes a heteroclinic bifurcation at $\alpha = 0$.

**(5) (Asymptote of the period)** Find an asymptotic form of the cycle period $T(\beta)$ near the homoclinic bifurcation on the plane. Is this result valid for the $n$-dimensional case? (*Hint*: Use the fact that a point on the cycle spends the most time near the saddle.)

**(6) (Multiplier of the cycle near homoclinic bifurcation)** Show that the (nontrivial) multiplier of the cycle bifurcating from a homoclinic orbit in a planar system approaches zero as $\beta \to 0$. Can this result be generalized to higher dimensions?

**(7) ($C^1$-linearization near the saddle on the plane)**

(a) Draw *isochrones*, $\tau_{1,2} = \text{const}$, of constant "exit" times from the unit square $\Omega$ for the linear system (6.7). Check that these lines are transversal. How will the figure change in the nonlinear case? Prove that the map $\Phi(y)$ constructed in the proof of Theorem 6.1 is a homeomorphism.

(b) Prove that the map $\Phi(y)$ has only first-order continuous partial derivatives at $y = 0$. (*Hint*: $\Phi_y(0) = I$, see Deng [1989].)

**(8) (Dependence of orbits upon a singular parameter)** Consider the following slow-fast system:

$$\begin{cases} \dot{x} &= x^2 - y, \\ \dot{y} &= -\varepsilon, \end{cases}$$

where $\varepsilon$ is small but positive. Take an orbit of the system starting at

$$\begin{aligned} x_0 &= -(1+\varepsilon), \\ y_0 &= 1. \end{aligned}$$

Let $y_1 = y_1(\varepsilon)$ be the ordinate of the point of intersection between the orbit and the vertical line $x = 1$.

(a) Show that the derivative of $y_1(\varepsilon)$ with respect to $\varepsilon$ tends to $-\infty$ as $\varepsilon \to 0$. (*Hint:* $y_1'(\varepsilon) = -T(\varepsilon)$, where $T$ is the "flight" time from the initial point $(x_0, y_0)$ to the point $(1, y_1)$.)

(b) Check that the result will not change if we take $x_0 = -(1 + \varphi(\varepsilon))$ with any smooth positive function $\varphi(\varepsilon) \to 0$ for $\varepsilon \to 0$.

(c) Explain the relationship between the above results and nondifferentiability of the split function in the slow-fast planar system used as the example in Section 2.

(d) Prove that, actually, $y_1(\varepsilon) \sim \varepsilon^{2/3}$. (*Hint:* See Mishchenko & Rozov [1980].)

**(9) (Strong inclination property)** Consider a system that is linear,

$$\begin{cases} \dot{x_1} &= \lambda_1 x_1, \\ \dot{x_2} &= \lambda_2 x_2, \\ \dot{x_3} &= \lambda_3 x_3, \end{cases}$$

where $\lambda_1 > 0 > \lambda_2 > \lambda_3$, inside the unit cube $\Omega = \{(x_1, x_2, x_3) : -1 \leq x_i \leq 1,\ i = 1, 2, 3\}$. Let $\varphi^t$ denote its evolution operator (flow).

(a) Take a line $l_0$ within the plane $x_1 = 1$ passing through the $x_1$-axis and show that its image under the flow (i.e., $l(t) = \varphi^t l$ with $t < 0$) is also a line in some plane $x_1 = \text{const}$ passing through the same axis.

(b) Show that the limit

$$\lim_{t\to-\infty} \varphi^t l$$

is the same for all initial lines except the line $l_0 = \{x_1 = 1\} \cap \{x_3 = 0\}$. What is the limit?

(c) Assume that the system outside the cube $\Omega$ possesses an orbit that is homoclinic to the origin. Using part (b), show that generically the stable manifold $W^s(0)$ intersects itself along the nonleading eigenspace $x_1 = x_2 = 0$. Reformulate the genericity condition as the condition of transversal intersection of $W^s(0)$ with some other invariant manifold near the saddle.

(d) Sketch the shape of the stable manifold in the degenerate case. Guess which phase portraits can appear under perturbations of this degenerate system. (*Hint:* See Yanagida [1987], Deng [1993*a*].)

**(10) (Proofs of Theorems 6.2–6.4 revisited)**

(a) Compute the near-to-saddle map $\Delta$ in the saddle and saddle-focus cases in $\mathbb{R}^3$ assuming that the system is linear inside the unit cube $\Omega = \{(x_1, x_2, x_3) : -1 \le x_i \le 1,\ i = 1, 2, 3\}$ and the equilibrium point is located at the origin.

(b) Write a general form of the linear part of the global map $Q : (x_2, x_3) \mapsto (x_1, x_3)$ using the split function as a parameter. How does the formula reflect the twisting of the orbit that is homoclinic to the saddle?

(c) Compose a superposition of the maps defined in parts (a) and (b) of the exercise and write the system of equations for its fixed points in the saddle and saddle-focus cases. Analyze the solutions of this system by reducing it to a scalar equation for the $x_1$-coordinate of the fixed points.

**(11)** Show that the saddle quantity $\sigma_0$ of the equilibrium in the wave system for the FitzHugh-Nagumo model is positive. (*Hint*: $\sigma_1 = \lambda_1 + \lambda_2 + \lambda_3 = c > 0$.)

**(12) (Singular homoclinic in $\mathbb{R}^3$)**

(a) Check that the following slow-fast system (cf. Deng [1994]),

$$\begin{cases} \dot{x} &= (z+1) + (1-z)[(x-1) - y], \\ \dot{y} &= (1-z)[(x-1) + y], \\ \varepsilon\dot{z} &= (1-z^2)[z + 1 - m(x+1)] - \varepsilon z, \end{cases}$$

has a homoclinic orbit to the equilibrium $(1, 0, -1)$ in the *singular* limit $\varepsilon = 0$, provided $m = 1$. (*Hint:* First, formally set $\varepsilon = 0$ and analyze the equations on the *slow* manifolds defined by $z = \pm 1$. Then plot the shape of the surface $\dot{z} = 0$ for small but positive $\varepsilon$.)

(b) Could you prove that there is a continuous function $m = m(\varepsilon)$, $m(0) = 1$, defined for $\varepsilon \ge 0$, such that for the corresponding parameter value the system has a saddle-focus with a homoclinic orbit for small $\varepsilon > 0$? What is

the sign of the saddle quantity? How many periodic orbits we one expect near the bifurcation?

(c) If part (b) of the exercise is difficult for you, try to find the homoclinic orbit numerically using the boundary-value method described in Chapter 10 and the singular homoclinic orbit from part (a) as the initial guess.

**(13) (Melnikov integral)** Prove that the Melnikov integral (6.25) is nonzero for the homoclinic orbit $\Gamma_0$ in the system (6.8) from Example 6.1. (*Hint:* Find $t_\pm = t_\pm(x)$ along the upper and lower halfs of $\Gamma_0$ by integrating the first equation of (6.8). Then transform the integral (6.25) into the sum of two integrals over $x \in [0, 1]$.)

## 6.6 Appendix 1: Focus-focus homoclinic bifurcation in four-dimensional systems

In this appendix we study dynamics of four-dimensional systems near an orbit homoclinic to a hyperbolic equilibrium with two complex pairs of eigenvalues (*focus-focus*). This case is similar to the saddle-focus homoclinic case.

Consider a system

$$\dot{x} = f(x, \alpha), \quad x \in \mathbb{R}^4, \ \alpha \in \mathbb{R}^1, \tag{A.1}$$

where $f$ is a smooth function. Assume that at $\alpha = 0$ the system has a hyperbolic equilibrium $x_0 = 0$ with two pairs of complex eigenvalues, namely,

$$\lambda_{1,2}(0) = \rho_1(0) \pm i\omega_1(0), \quad \lambda_{3,4}(0) = \rho_2(0) \pm i\omega_2(0),$$

where

$$\rho_1(0) < 0 < \rho_2(0), \ \omega_{1,2}(0) > 0,$$

(see Figure 6.43). Generically, the *saddle quantity* is nonzero:

(H.1) $\sigma_0 = \rho_1(0) + \rho_2(0) \neq 0.$

Actually, only the case

$$\sigma_0 = \rho_1(0) + \rho_2(0) < 0$$

will be treated, because we can reverse time otherwise. Since $\lambda = 0$ is not an eigenvalue of the Jacobian matrix $f_x(x_0, 0)$, the Implicit Function Theorem guarantees the persistence of a close hyperbolic equilibrium with two pairs of complex eigenvalues for all sufficiently small $|\alpha|$. Assuming that the origin of coordinates is already shifted to this equlibrium, we can write $(A.1)$ in the form

$$\dot{x} = A(\alpha)x + F(x, \alpha), \tag{A.2}$$

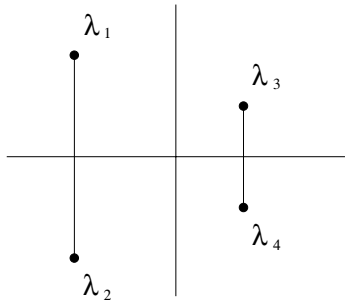


FIGURE 6.43. Eigenvalues of a focus-focus.

where $F = O(\|x\|^2)$ and the matrix $A(\alpha)$ has the eigenvalues

$$\lambda_{1,2}(\alpha) = \rho_1(\alpha) \pm i\omega_1(\alpha), \quad \lambda_{3,4}(\alpha) = \rho_2(\alpha) \pm i\omega_2(\alpha),$$

with $\rho_i(0),\ \omega_i(0)$ satisfying the imposed conditions.

The focus-focus equilibrium has the two-dimensional stable and unstable manifolds $W^{s,u}$ that can be globally extended. Suppose that at $\alpha = 0$ the manifolds $W^u$ and $W^s$ intersect along a homoclinic orbit $\Gamma_0$. We assume that the intersection of the tangent spaces to the stable and unstable manifolds is one-dimensional at any point $x \in \Gamma_0$:[9]

(H.2) $\dim\,(T_x W^u \cap T_x W^s) = 1.$

This condition holds generically for systems with a homoclinic orbit to a hyperbolic equilibrium.

The following theorem by Shil'nikov is valid.

**Theorem 6.11** *For any system* (A.2)*, having a focus-focus equilibrium point $x_0$ with a homoclinic orbit $\Gamma_0$ at $\alpha = 0$ and satisfying the nondegeneracy conditions* (H.1) *and* (H.2)*, there exists a neighborhood $U_0$ of $\Gamma_0 \cup x_0$ in which the system has an infinite number of saddle limit cycles in $U_0$ for all sufficiently small $|\alpha|$.* □

**Sketch of the proof:**

First consider the case $\alpha = 0$. Write the system (A.2) in its real eigenbasis. This can be done by applying to (A.2) a nonsingular linear transformation putting $A$ in its real Jordan form. In the eigenbasis, the system at $\alpha = 0$ will take the form

$$\begin{cases} \dot{x}_1 &= \rho_1 x_1 - \omega_1 x_2 + G_1(x), \\ \dot{x}_2 &= \omega_1 x_1 + \rho_1 x_2 + G_2(x), \\ \dot{x}_3 &= \rho_2 x_3 - \omega_2 x_4 + G_3(x), \\ \dot{x}_4 &= \omega_2 x_3 + \rho_2 x_4 + G_4(x), \end{cases} \tag{A.3}$$

[9]This intersection is spanned by the phase velocity vector $f(x, 0)$ for $x \in \Gamma_0$.

where old notations for the phase variable are preserved and $G = O(\|x\|^2)$. Now introduce new coordinates $y$ that locally linearize the system (A.3). Due to a theorem by Belitskii (see Appendix 2) there exists a nonlinear transformation

$$y = x + g(x),$$

where $g$ is a $C^1$ function ($g_x(0) = 0$), that locally conjugates the flow corresponding to (A.3) with the flow generated by the linear system:

$$\left\{\begin{array}{lcl} \dot{y}_1 &=& \rho_1 y_1 - \omega_1 y_2, \\ \dot{y}_2 &=& \omega_1 y_1 + \rho_1 y_2, \\ \dot{y}_3 &=& \rho_2 y_3 - \omega_2 y_4, \\ \dot{y}_4 &=& \omega_2 y_3 + \rho_2 y_4. \end{array}\right. \tag{A.4}$$

In the coordinates $y \in \mathbb{R}^4$ the unstable manifold $W^u$ is locally represented by $y_1 = y_2 = 0$, while the stable manifold $W^s$ is given by $y_3 = y_4 = 0$. Suppose that the linearization (A.4) is valid in the unit 4-cube $\{|y_i| \le 1,\ i = 1, 2, 3, 4\}$ which can always be achieved by a linear scaling.

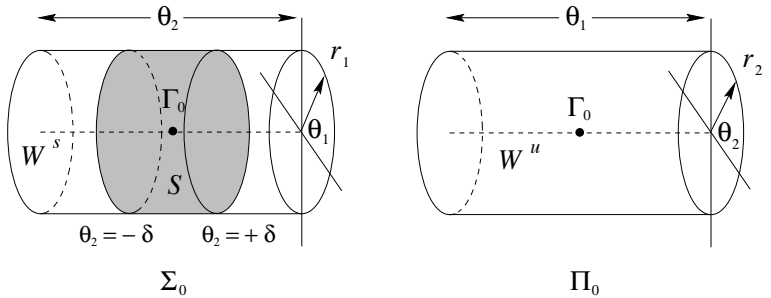


FIGURE 6.44. Cross-sections $\Sigma_0$ and $\Pi_0$.

Write (A.4) in the polar coordinates

$$\left\{\begin{array}{lcl} \dot{r}_1 &=& \rho_1 r_1, \\ \dot{\theta}_1 &=& \omega_1, \\ \dot{r}_2 &=& \rho_2 r_2, \\ \dot{\theta}_2 &=& \omega_2, \end{array}\right. \tag{A.5}$$

by substituting

$$y_1 = r_1 \cos\theta_1,\ y_2 = r_1 \sin\theta_1,\ y_3 = r_2 \cos\theta_2,\ y_4 = r_2 \sin\theta_2.$$

Introduce two *three-dimensional* cross-sections for (A.5):

$$\begin{array}{lcl} \Sigma &=& \{(r_1, \theta_1, r_2, \theta_2) : r_2 = 1\}, \\ \Pi &=& \{(r_1, \theta_1, r_2, \theta_2) : r_1 = 1\}, \end{array}$$

and two submanifolds within these cross-sections, namely:

$$\begin{aligned}\Sigma_0 &= \{(r_1,\theta_1,r_2,\theta_2) : r_1 \le 1,\ r_2 = 1\} \subset \Sigma,\\ \Pi_0 &= \{(r_1,\theta_1,r_2,\theta_2) : r_1 = 1,\ r_2 \le 1\} \subset \Pi.\end{aligned}$$

$\Sigma_0$ and $\Pi_0$ are three-dimensional solid tori that can be vizualized as in Figure 6.44, identifying the left and the right faces. The stable manifold $W^s$ intersects $\Sigma_0$ along the center circle $r_1 = 0$, while the unstable manifold $W^u$ intersects $\Pi_0$ along the center circle $r_2 = 0$. Without loss of generality, assume that the homoclinic orbit $\Gamma_0$ crosses $\Sigma_0$ at the point with $\theta_1 = 0$, while its intersection with $\Pi_0$ occurs at $\theta_2 = 0$.

As usual, define a Poincaré map $P : \Sigma \to \Sigma$ along the orbits of the system and represent this map as a superposition $P = Q \circ \Delta$ of two maps: a near-to-saddle map $\Delta : \Sigma \to \Pi$ and a map $Q : \Pi \to \Sigma$ near the global part of the homoclinic orbit $\Gamma_0$. Now introduce a three-dimensional solid cylinder $S \subset \Sigma_0$

$$S = \{(r_1,\theta_1,r_2,\theta_2) :\ r_1 \le 1,\ r_2 = 1,\ -\delta \le \theta_2 \le \delta\}$$

with some $\delta > 0$ fixed (see Figure 6.44), and trace its image under the Poincaré map $P$.

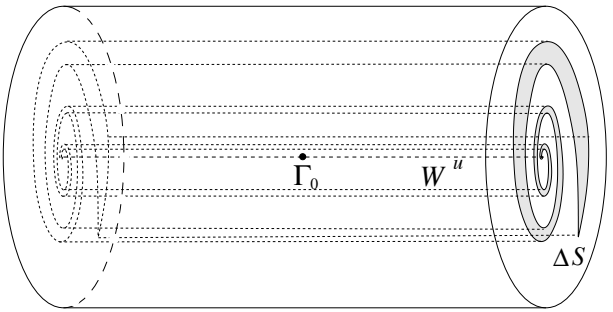


FIGURE 6.45. The image $\Delta S$ in $\Pi_0$.

The map $\Delta : \Sigma \to \Pi$ can be computed explicitly using (A.5). Namely,

$$\Delta : \begin{pmatrix} r_1 \\ \theta_1 \\ 1 \\ \theta_2 \end{pmatrix} \mapsto \begin{pmatrix} 1 \\ \theta_1 + \frac{\omega_1}{\rho_1} \ln \frac{1}{r_1} \\ r_1^{-\frac{\rho_2}{\rho_1}} \\ \theta_2 + \frac{\omega_2}{\rho_1} \ln \frac{1}{r_1} \end{pmatrix}, \tag{A.6}$$

since the flight time from $\Sigma$ to $\Pi$ is equal to

$$T = \frac{1}{\rho_1} \ln \frac{1}{r_1}.$$

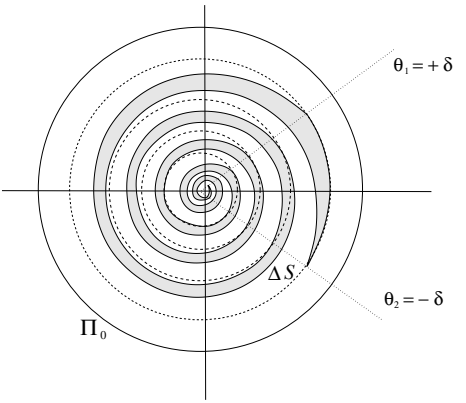


FIGURE 6.46. The section of $\Delta S$ by the plane $\theta_1 = 0$.

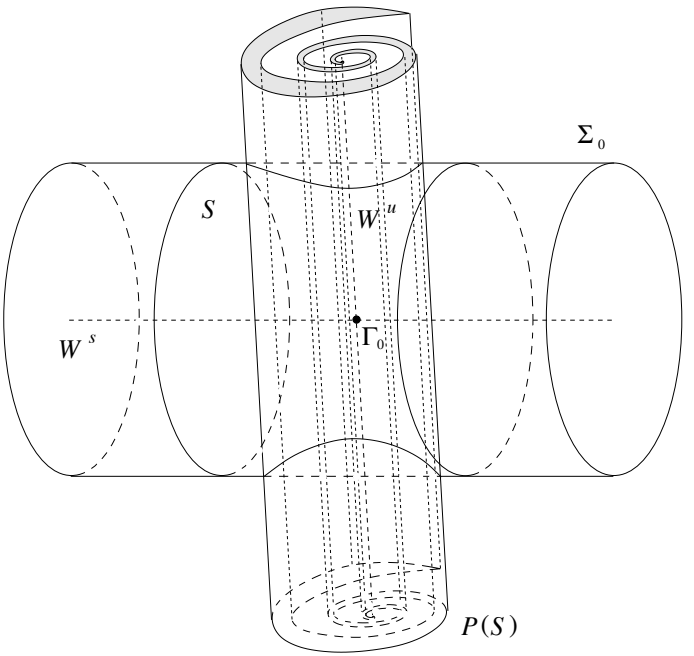


FIGURE 6.47. The image $P(S)$ and the preimage $S$ in $\Sigma$.

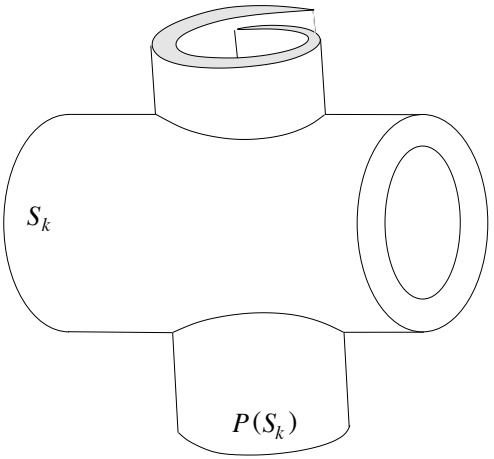


FIGURE 6.48. The image $P(S_k)$ and the preimage $S_k$ in $\Sigma$.

According to (A.6), the image $\Delta S \subset \Pi_0$ is a solid *"toroidal scroll"* sketched in Figure 6.45. The section of the image by the plane $\theta_2 = 0$ is presented in Figure 6.46.

The $C^1$ map $Q : \Pi \to \Sigma$ places the scroll back into the cross-section $\Sigma$ by rotating and deforming it such that the image $Q(\Delta S)$ cuts through the cylinder $S$ (see Figure 6.47). The center circle $r_2 = 0$ of $\Pi_0$ is transformed by $Q$ into a curve intersecting the center circle $r_1 = 0$ of $\Sigma_0$ at a nonzero angle due to the condition (H.2).

The geometry of the constructed Poincaré map $P$ implies the presence of three-dimensional analogs of Smale's horseshoe. Indeed, let us partition $S$ into a series of solid annuli: $S = \cup_{k=0}^{\infty} S_k$, where

$$S_k = \left\{ (r_1, \theta_1, r_2, \theta_2) : e^{-\frac{2\pi(k+1)\rho_2}{\omega_1}} < r_1 \le e^{-\frac{2\pi k \rho_2}{\omega_1}},\ r_2 = 1,\ |\theta_2| \le \delta \right\}.$$

Provided $k$ is sufficiently large, $S_k$ is mapped by $P$ into a "one-turn scroll" $P(S_k)$ that intersects $S_k$ by two disjoint domains (see Figure 6.48). This is a key feature of Smale's example. Thus, at $\alpha = 0$, the system (A.1) has an infinite number of Smale's horseshoes, each of them implying the existence of a Cantor invariant set containing an infinite number of saddle limit cycles.

If $|\alpha|$ is small but nonzero, the above construction can still be carried out. However, generically, the manifolds $W^s$ and $W^u$ split by $O(\alpha)$ distance, so the image of the center circle of $\Pi_0$ does not intersect that of $\Sigma_0$. Thus, only a finite number of the three-dimensional horseshoes remain. Nevertheless, they still give an infinite number of cycles near $\Gamma_0$.

## 6.7 Appendix 2: Bibliographical notes

The homoclinic orbit bifurcation in planar dynamical systems was analyzed by Andronov & Leontovich [1939] (an exposition with much detail can be found in Andronov et al. [1973]). $C^1$-linearization was not known to Andronov; therefore he had to give delicate estimates for the near-to-saddle map (see Wiggins [1988] for such estimates in the $n$-dimensional case). $C^k$-linearization near a hyperbolic equilibrium is studied by Sternberg [1957] and Belitskii [1973, 1979], as well as by many other authors. A theorem by Belitskii provides the $C^1$-equivalence of the flow corresponding to a system in $\mathbb{R}^n$ to the flow generated by its linear part near a hyperbolic equilibrium with eigenvalues $\lambda_1, \lambda_2, \ldots, \lambda_n$ such that

$$\text{Re } \lambda_i \neq \text{Re } \lambda_j + \text{Re } \lambda_k$$

for all combinations of $i, j, k = 1, 2, \ldots, n$. An elementary proof of $C^1$-linearization near a hyperbolic saddle on the plane, which is reproduced in the proof of Theorem 6.1, is due to Deng [1989].

Integrals over homoclinic orbits characterizing splitting of invariant manifolds first appeared in the paper by Melnikov [1963] devoted to *periodic perturbations* of planar autonomous systems. If the unperturbed system has a homoclinic orbit to a saddle equilibrium, the perturbed system (considered as an autonomous system in $\mathbb{R}^2 \times \mathbb{S}^1$) will have a saddle limit cycle with two-dimensional stable and unstable invariant manifolds. These manifolds could intersect along orbits homoclinic to the cycle, giving rise to the Poincaré homoclinic structure and associated chaotic dynamics (see Chapter 2). In a fixed cross-section $t = t_0$, the points corresponding to a homoclinic orbit can be located near the unperturbed homoclinic loop as zeros of the so-called *Melnikov function* (see details in Sanders [1982], Guckenheimer & Holmes [1983], Wiggins [1990]). The generalization of Melnikov's technique to $n$-dimensional situations using the variational and adjoint variational equations is due to Palmer [1984] (see also Lin [1990]). In the papers by Beyn [1990*b*, 1990*a*] the equivalence of the transversality of the intersection of the stable and unstable manifolds in the extended system (6.20) to the nonvanishing of the Melnikov integral (6.24) is proved.

Bifurcations of phase portraits near orbits homoclinic to a hyperbolic equilibrium in $n$-dimensional autonomous systems were first studied by Shil'nikov [1963] and Neimark & Shil'nikov [1965] under simplifying assumptions. The general theory has been developed by Shil'nikov [1968, 1970] (there are also two preceding papers by him in which three- and four-dimensional cases were analyzed: Shil'nikov [1965, 1967*a*]). The main tool of his analysis is a representation of the near-to-saddle map as the solution to a boundary-value problem (the so-called *parametric representaion*), see Deng [1989] for the modern treatment of this technique. This parametrization allowed Shil'nikov to prove one-to-one correspondence between the saddle cycles and periodic sequences of symbols. A particular feature that

makes Shil'nikov's main papers difficult to read is the absence of figures. For example, the notion of "orientation" or "twisting" never appeared in his original papers explicitly (it is hidden in the signs of some indirectly defined determinants). A geometrical treatment of the saddle-focus case in $\mathbb{R}^3$ can be found in Guckenheimer & Holmes [1983] and Tresser [1984]. In the later paper the $C^1$-linearization near the saddle-focus is used. Wiggins [1988, 1990] gives many details concerning homoclinic bifurcations in $\mathbb{R}^3$ and $\mathbb{R}^4$. Appendix 1 follows his geometrical approach to the focus-focus homoclinic bifurcation.

Arnol'd et al. [1994] provide an excellent survey of codimension 1 homoclinic bifurcations. It includes a proof of topological invariance of $\nu_0$, as well as the construction of topological normal forms for the saddle homoclinic bifurcation.

The bifurcations of the "basic" limit cycle near an orbit homoclinic to the saddle-focus were studied by Gaspard [1983], Gaspard, Kapral & Nicolis [1984], and Glendinning & Sparrow [1984]. The existence of the secondary homoclinic orbits is proved by Evans et al. [1982]. Actually, basic results concerning these bifurcations follow from the analysis of a codim 2 bifurcation performed by Belyakov [1980], who studied the homoclinic bifurcation in $\mathbb{R}^3$ near the saddle to saddle-focus transition (see also Belyakov [1974, 1984] for the analysis of other codim 2 saddle-focus cases). Codim 2 homoclinic bifurcations in $\mathbb{R}^3$ have recently attracted much interest (see, e.g., Nozdrachova [1982], Yanagida [1987], Glendinning [1988], Chow, Deng & Fiedler [1990], Kisaka, Kokubu & Oka [1993*a*, 1993*b*], Hirschberg & Knobloch [1993], Deng [1993*a*], Homburg, Kokubu & Krupa [1994], and Deng & Sakamoto [1995]).

Homoclinic bifurcations in $n$-dimensional cases with $n > 4$ were treated in the original papers by Shil'nikov and by Ovsyannikov & Shil'nikov [1987] (see also Deng [1993*b*]). The existence of $C^{k,\beta}$ center manifolds near homoclinic bifurcations in $n$-dimensional systems have been established by Sandstede [1993, 1995] and Homburg [1993].

There is an alternative method to prove the bifurcation of a periodic orbit from the homoclinic orbit: a function space approach based on the Lyapunov-Schmidt method [Lin 1990].

Homoclinic bifurcations in planar slow-fast systems were treated by Diener [1983] in the framework of nonstandard analysis. An elementary treatment of the planar case is given by Kuznetsov, Muratori & Rinaldi [1995] with application to population dynamics. Some higher-dimensional cases have been considered by Szmolyan [1991]. Many examples of three-dimensional slow-fast systems that exhibit homoclinic bifurcations are constructed by Deng [1994].

Explicit examples of two- and three-dimensional systems having algebraic homoclinic orbits of codim 1 and 2 have been presented by Sandstede [1997*a*].